

Journal Pre-proofs

A comprehensive molecular phylogeny of Afrotropical white-eyes (Aves: Zosteropidae) highlights prior underestimation of mainland diversity and complex colonisation history

Frederico C. Martins, Siobhan C. Cox, Martin Irestedt, Robert P. Prÿs-Jones nvestigation, Julia J. Day

PII: S1055-7903(20)30115-9
DOI: <https://doi.org/10.1016/j.ympev.2020.106843>
Reference: YMPEV 106843

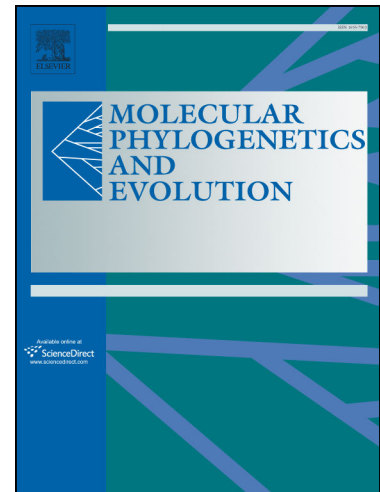
To appear in: *Molecular Phylogenetics and Evolution*

Received Date: 16 September 2019
Revised Date: 7 April 2020
Accepted Date: 16 April 2020

Please cite this article as: Martins, F.C., Cox, S.C., Irestedt, M., Prÿs-Jones nvestigation, R.P., Day, J.J., A comprehensive molecular phylogeny of Afrotropical white-eyes (Aves: Zosteropidae) highlights prior underestimation of mainland diversity and complex colonisation history, *Molecular Phylogenetics and Evolution* (2020), doi: <https://doi.org/10.1016/j.ympev.2020.106843>

This is a PDF file of an article that has undergone enhancements after acceptance, such as the addition of a cover page and metadata, and formatting for readability, but it is not yet the definitive version of record. This version will undergo additional copyediting, typesetting and review before it is published in its final form, but we are providing this version to give early visibility of the article. Please note that, during the production process, errors may be discovered which could affect the content, and all legal disclaimers that apply to the journal pertain.

Elsevier Inc.



Running title: Molecular phylogeny of Afrotropical Zosteropidae

A comprehensive molecular phylogeny of Afrotropical white-eyes (Aves: Zosteropidae) highlights prior underestimation of mainland diversity and complex colonisation history

Frederico C. Martins^a, Siobhan C. Cox^{a,b}, Martin Irestedt^c, Robert P. Prÿs-Jones^b, Julia J. Day^{a,1}

^aDepartment of Genetics, Evolution and Environment, University College London, Gower Street, London WC1E 6BT, U.K.

^bBird Group, Department of Life Sciences, The Natural History Museum, Akeman Street, Tring, Herts HP23 6AP, U.K.

^cDepartment of Bioinformatics and Genetics, Swedish Museum of Natural History, PO Box 50007, Stockholm 10405, Sweden

¹ Corresponding author E-mail: j.day@ucl.ac.uk

Abstract

White-eyes (*Zosterops*) are a hyper-diverse genus of passerine birds that have rapidly radiated across the Afrotropics and Southeast Asia. Despite their broad range, a disproportionately large number of species are currently recognised from islands compared to the mainland. Described species-level diversity of this ‘great speciator’ from continental Africa-Arabia is strikingly low, despite the vast size and environmental complexity of this region. However, efforts to identify natural groups using traditional approaches have been hindered by the remarkably uniform morphology and plumage of these birds. Here, we investigated the phylogenetic relationships and systematics of Afrotropical *Zosterops*, including the Gulf of Guinea and western Indian Ocean islands. We included exceptional sampling (~160 individuals) from all except one

subspecies of the 54 taxa (31 species, plus 22 additional named sub-species) currently recognized throughout the region, in addition to a subset of extra-Afrotropical taxa, by exploiting blood and archival samples. Employing a multi-locus phylogenetic approach and applying quantitative species delimitation we tested: 1) if there has been a single colonisation event of the Afrotropical realm; 2) if constituent mainland and island birds are monophyletic; and 3) if mainland diversity has been underestimated. Our comprehensive regional phylogeny revealed a single recent colonisation of the Afrotropical realm *c.* 1.30 Ma from Asia, but a subsequent complex colonisation history between constituent island and mainland lineages during their radiation across this vast area. Our findings suggest a significant previous underestimation of continental species diversity and, based on this, we propose a revised taxonomy. Our study highlights the need to densely sample species diversity across ranges, providing key findings for future conservation assessments and establishing a robust framework for evolutionary studies.

Key words: cryptic species; islands; continents; Passeriformes; species delimitation; *Zosterops*.

Introduction

The hyper-diverse family Zosteropidae (Aves: Passeriformes) is best known for its exceptional colonisation abilities (Diamond et al., 1976; Melo et al., 2011; Phillimore et al., 2008; Slikas et al., 2000; Warren et al., 2006), which has led to its broad distribution across sub-Saharan Africa, the Arabian peninsula, southern and eastern Asia (from the Indian subcontinent through to Japan) and Australasia, as well as islands of the Indian Ocean, western Pacific Ocean and the Gulf of Guinea regions (van Balen, 2019). A disproportionate number of zosteropid species are currently described from islands compared to the mainland (~90% from islands), having colonised more islands worldwide than any other passerine group (Moreau, 1957). The family is composed of small (typically 10-12 cm), arboreal, gregarious birds, in which 72% of all recognised species (97/135 species) are placed within the genus *Zosterops*, commonly referred to as white-eyes (van Balen, 2019).

The remarkably uniform appearance of *Zosterops* (Appendix A Plates A-C), apart from some aberrant island forms (Melo et al., 2011), has greatly complicated efforts to identify natural groups (Mayr, 1965; Moreau, 1957). Morphology (including plumage) and distribution have guided much of the current taxonomy, supported by details on general behaviour, nesting, and vocalisations. The use of plumage colouration as a taxonomic character has received considerable attention and has been used widely as a tool for facilitating taxonomic arrangements (Mees, 1957, 1961, 1969; Moreau, 1967). However, while these birds possess relatively simple plumage patterns, the distribution and gradation of colouration between forms appears to change readily (van Balen, 2019). Despite this, in many cases plumage variation has provided the primary characters for species delimitation (van Balen, 2019). Morphological variation across the range of the family Zosteropidae is also slight, and characteristics such as body size and wing length can often be linked to abiotic variables such as altitude and temperature (Moreau, 1957), thus making them unreliable for species delimitation. As a result, although there were extensive pre-molecular studies of the group - by Moreau (1957) for western Zosteropidae, and Mayr (1965) and Mees (1957, 1961, 1969) for eastern Zosteropidae - the affinities of numerous taxa remained unresolved.

With their seemingly greater prevalence on oceanic islands, it is no surprise that island *Zosterops* have received greater attention in evolutionary studies. This is true for the Afrotropical realm, as while the systematics of *Zosterops* from the western Indian Ocean (Warren et al., 2006) and Gulf of Guinea (Melo et al., 2011) regions have greatly benefited from recent molecular insights, limited sampling across mainland Africa has hindered more broad scale assessments of species validity in this region. This is unsurprising given that by traditional assessments more than half the African *Zosterops* species are offshore island endemics, and until recently there were only four described species restricted to mainland Africa (Dickinson, 2003). Recent molecular studies of African mainland taxa (Cox et al., 2014; Habel et al., 2015; Oatley et al., 2012) have started to address this imbalance and shown that traditional taxonomic approaches based on plumage (Moreau, 1957) have led to some erroneous taxonomic groupings. Based on their findings, Cox et al. (2014) suggested that most East African montane subspecies of *Zosterops poliogastrus* be elevated to species status. A previous taxonomic review by Pearson and Turner (2017), which

incorporated the findings from Cox's (2013) unpublished thesis recognised ten mainland East African species. Currently 14 African mainland *Zosterops* species are recognized (van Balen, 2019), although the species status of these birds has not been investigated using quantitative molecular methods.

In this study we included exceptional coverage of taxa across sub-Saharan Africa, the Arabian Peninsula, Gulf of Aden, Gulf of Guinea and western Indian Ocean islands, exploiting archival and blood samples, to generate a comprehensive multi-locus phylogeny for the Afrotropical realm. We addressed the following questions: 1) Was there a single colonisation event of the Afrotropical realm? 2) Are constituent mainland and island birds monophyletic? and 3) Has mainland diversity has been underestimated? Based on our results we suggest a revised taxonomy for mainland taxa, thereby increasing species diversity to a similar level as for island taxa in this region.

2. Materials and methods

2.1 Taxon sampling

Our study included comprehensive coverage of all currently recognised taxa across sub-Saharan Africa, the southern Arabian Peninsula, Gulf of Aden, and the Gulf of Guinea and Indian Ocean islands (Fig. 1A,B) representing all except one subspecies (*Z. maderaspatanus menaiensis*) of the 54 Afrotropical taxa (31 species, plus 22 additional named sub-species) (van Balen, 2019) greatly increasing sampling from previous studies (Cox et al., 2014; Melo et al., 2011; Warren et al., 2006). We included coverage of all 14 *Zosterops* species and 18 sub-species recognized from the African mainland (van Balen, 2019). In addition, the 18 recognised species (including the extinct *Z. semiflavus*) from the western Indian Ocean and Gulf of Guinea island systems and four of the five sub-species from these systems were included. A further ten *Zosterops* taxa from Asia and Indo-Pacific were selected as outgroups (Fig. 1B), which included a subspecies of *Z. palpebrosus* (*Z. p. siamensis* AMNH DOT6512, AMNH DOT2659, see Table 1), reassigned from its original identification as *Z. japonicus* based on the study of Lim et al. (2019), along with the more distantly related Chestnut-faced Babbler (*Zosterornis whiteheadi*) based on previous studies (Moyle et al., 2012; Moyle et al., 2009). In total, 161 specimens were included (Table 1; see also Appendix A, Plates A-C for representatives

of these taxa). Novel sequence data (Appendix B, Table S1) were generated from 63 museum specimens (specimen collection dates ranged from 1899 to 2008), of which 19 were excluded due to poor quality sequence data, and 50 blood samples. A further 48 Genbank sequences were used in this study (Cox et al., 2014; Li et al., 2016 ; Melo et al., 2011; Moyle et al., 2012; Moyle et al., 2009; Warren et al., 2006; Zuccon and Ericson, 2012) (Appendix B, Table S1). Where possible three individuals per subspecies for all mainland African members were sampled to ensure coverage of their geographic range, but ≤ 2 for the following taxa: *Z. a. arabs* (n=2), *Z. [p] kaffensis* (n=2), *Z. s. demeryi* (n=1), *Z. s. gerhardi* (n=1), *Z. s. kasaicus* (n=1), *Z. s. quanzae* (n=2), *Z. s. reichenowi* (n=1), *Z. s. stuhlmanni* (n=2), *Z. s. tongensis* (n=1) and *Z. s. toroensis* (n=1).

2.2 Molecular markers and primers

Sequence data were generated for three mitochondrial (mt)DNA loci: NADH dehydrogenase subunit III (ND3, 348 bp), cytochrome b (Cyt b, 1113 bp) and ATP synthase 6 (ATP6, 661bp), which have previously been used in *Zosterops* studies (Warren et al., 2006; Melo et al. 2011; Cox et al., 2014). In addition, five nuclear (nu)DNA introns: Transforming growth factor-beta 2 intron 5 (TGF β 2, 582bp), Glyceraldehyde 3-phosphate dehydrogenase intron 11 (G3PDH, 332bp), Fibrinogen intron 7 (Fib 7, 695bp), and the two sex-linked loci on the avian Z-chromosome: Chromodomain helicase DNA binding protein 1 (CHD1, 476bp) and the Muscle-specific kinase, intron 3 (MUSK, 574bp), were selected based on their utility in previous avian studies investigating recent clades (Batalha-Filho et al., 2014; Oatley et al., 2012; Rocha et al., 2015). We sequenced mitochondrial genes Cyt b and ND3 (for all samples), ATP6 (for blood samples only) and nuclear introns (for a subset of blood samples, see Appendix B) in an attempt to provide better resolution at deeper nodes. We amplified molecular markers using published primers (Appendix B, Table S2) and designed a series of new primers for amplifying and sequencing DNA from archival samples using the program Primer 3 v.0.4. In an attempt to obtain greater amounts of sequence data, we also designed eight primer sets to break down the Cyt b and ND3 genes into a series of smaller overlapping fragments (150–250 bp) (Appendix B, Table S3). All sequences have been deposited in Genbank (see Appendix B, Table S1).

2.3 DNA extraction

We extracted total DNA from blood samples using the standard protocol of DNeasy Blood and tissue kit (Qiagen, UK). To minimise damage to museum specimens, a small tissue sample was taken from the proximal phalanx (large toe pad) on the hind digit as the source for DNA extraction, following Mundy et al. (1997). Contamination was avoided by taking tissue samples from each specimen using sterile scalpels and forceps. Dried toe-pad samples were soaked in ddH₂O for 30 minutes to re-hydrate and extracted using the QIAamp DNA Micro kit (Qiagen). Adjustments to standard protocol included the addition of 20µl DTT (DL-Dithiothreitol) during tissue lysis. Two additional incubation steps were also included. Following the addition of buffer AL, lysates (digested products) were incubated at 72°C for 10 minutes to ensure optimal binding of DNA to the spin column membrane. Prior to elution of DNA, we added buffer AE to spin columns and incubated at room temperature for 15 minutes ensuring the highest possible yields of DNA. Extractions and amplification reactions were performed in rooms dedicated to working with archival and ancient material.

2.4 PCR amplification

PCR amplification of blood samples was conducted in 25µl reactions including 12.5µl MyTaq™ DNA Polymerase (BIOLINE), 9.5µl ddH₂O, 1µl primer (10mM) and 1µl template DNA. Amplification profiles of mt- and nuDNA markers are reported in Appendix B, Table S2. Purification of amplified PCR products was performed using Microclean and re-suspending DNA pellet in 5µl of water followed by cycle sequencing reaction with Big Dye Terminator v3.1.

PCR amplification of archival samples was also conducted in 25µl reactions, using puReTaq Ready-To-Go PCR Beads (GE Healthcare), which are pre-treated to minimise contamination. Single beads were combined with 21µl ddH₂O, 0.5µl of primer (10mM) and 3µl of template DNA. A hot-start touchdown PCR approach was used, where annealing temperatures for the first cycles were generally 1–2 °C below the T_m of primers. Given that primers were designed to have similar T_m 's, all reactions were run under the same

thermal cycling conditions (Appendix B, Table S3). Purification of amplified PCR products was performed using an ExoSAP-IT PCR Clean-up (GE Healthcare). ExoSAP-IT (5 μ l) was added directly to PCR products and incubated at 37°C for 30 minutes. Inactivation of ExoSAP-IT enzymes was performed by heating to 80°C for 15 minutes. Cycle sequencing reactions were performed in 20 μ l volumes using 1 μ l BigDye™ Terminator (PE Applied Biosystems), 4 μ l ABI sequencing buffer, 1 μ l primer (1.6 μ M), 2 μ l of the purified PCR product and 12 μ l of ddH₂O. Cycle sequencing reactions consisted of an initial denaturation at 96°C for 1 minute, followed by 25 cycles of 95°C for 30 seconds, 50°C for 15 seconds and 60°C for 4 minutes. Cycle sequencing products were purified using a DyeEX 96 kit cleanup (Qiagen) following standard protocols. All cleaned products from blood or archival samples were sequenced on an ABI 3730xl DNA analyser (Applied Biosystems, UK).

2.5 Sequence alignment and phylogenetic analyses

The software GENEIOUS v.6.0.6 (Biomatters) (Kearse et al., 2012) was used to visually check chromatograms for each primer pair before producing contigs of complementary fragments, which were then aligned using standard multiple GENEIOUS alignment. The concatenated gene sequences for some museum specimens have gaps or are slightly truncated as primer fidelity for these specimens was not always consistent across taxa.

Two matrices containing all 161 samples were assembled: 1) mitochondrial data (2122 bp) and 2) concatenating mitochondrial and nuclear data (4781 bp). PartitionFinder v.2.11 (Lanfear et al., 2012) was used to select the best-fit partitioning scheme, with 14 possible subsets defined (each codon position was defined for mtDNA protein-coding genes). The best scheme was calculated according to the Greedy algorithm using the Bayesian information criterion (BIC) (Table 2A).

Bayesian Inference (BI) and Maximum Likelihood (ML) were implemented using the models selected by PartitionFinder. Bayesian analysis was conducted using MrBayes v.3.2.6 (Ronquist and Huelsenbeck, 2003) using CIPRES (Miller et al., 2010). Base frequencies were estimated, and evolutionary rates were allowed to vary across partitions. For both matrices two independent analyses were run using Metropolis-Coupled

Markov Chain Monte Carlo (MCMCMC) chains for 5 million generations, sampling every 500 generations with a heating parameter of 0.1 and starting from a random tree. Stationarity of the Markov process was assessed graphically in TRACER v.1.7 (Rambaut et al., 2018), and all effective sample sizes (ESS) were >200. A burn-in of 10% was applied to the two independent replicates, with the final tree summarized and annotated from 18000 post burn-in trees using SumTrees v.4.0.0 (Sukumaran and Holder, 2010). Node support was assessed using Bayesian posterior probabilities (BPP). The ML tree search was performed on both datasets using GARLI (Genetic Algorithm for Rapid Likelihood Inference, v.2.01) (Zwickl, 2006). Node support for each dataset was ascertained with 100 non-parametric bootstraps (BS), and ML trees were summarized using a 50% majority-rule consensus tree in SumTrees.

2.6 Molecular dating analysis

Divergence times were estimated using BEAST v.2.4.8 (Bouckaert et al., 2014) implementing a relaxed lognormal molecular clock (Drummond et al., 2006) and using a Yule calibrated tree prior. Prior to running BEAST, a log-likelihood ratio test implemented in PAUP* v.4.0b10 (Swofford, 2002) rejected the null hypothesis of rate constancy ($-\ln L$ clock-enforced tree = 14814.81, $-\ln L$ unconstrained tree = 14636.92, d.f. = 158, $P < 0.05$). A single representative per species was chosen (incorporating species and potential candidate species based on our taxonomic recommendations, see Appendix A) in which samples were selected on having the highest coverage of sequence data available for mtDNA and nuclear loci. We ran the BEAST analysis using a constraint tree based on the topology generated from the Mr Bayes analysis (fully resolved tree) and removing multiple samples using the drop.tip function in Ape version 5.0 (Paradis et al., 2004) in R 3.4.3 (R Development Core Team, 2018). Following previous authors (Cox et al., 2014; Melo et al., 2011; Warren et al., 2006) a single geological calibration was enforced, assuming 0.5 million years to be the maximum age estimate for the volcanic origin of Grande Comore Island, and constraining the node that separates *Z. kirki* (formerly *Z. maderaspatanus kirki*) from other *Z. maderaspatanus* taxa applying a normal prior (0.5 ± 0.025). However, as there is a lack of resolution between several of these taxa, as previously shown (Cox et al., 2014; Warren et al., 2006), we follow these authors and place the calibration on the node

including all *Z. "maderaspatanus"* taxa (which includes *Z. kirki* and *Z. mayottensis*). Analyses were run unlinking mtDNA and nuDNA clocks, and unlinking site models based on the partitions from PartitionFinder (Table 2B). The MCMC analyses were run for 50 million generations for three independent runs using CIPRES (Miller et al., 2010), with trees and corresponding parameters sampled every 5,000 generations with a burn-in of 10%. Convergence of the MCMC runs was assessed graphically in TRACER v.1.7 ensuring all ESS >200 (Rambaut et al., 2018). The consensus trees were obtained from the post burn-in tree samples (rejecting the first 10%) using Tree Annotator v.2.4 and visualized using FigTree v1.4.3.

2.7 Mitochondrial DNA species delimitation

As the African mainland species referred to "*abyssinicus*" and "*senegalensis*" were found to be non-monophyletic, yet many subspecies were monophyletic (see results, Phylogenetic inference), we quantitatively delimited species applying the general mixed Yule-coalescent (GMYC) model (Fujisawa and Barraclough, 2013; Pons et al., 2006), which requires no prior assumptions regarding the probable placement of species boundaries (Powell, 2012). As an ultrametric tree is required for species delimitation analysis, the mtDNA dataset including all *Zosterops* samples (n=161) was analysed using BEAST v.2.4, applying the same settings as described above. GMYC examines transitions through time in tree-branching patterns between long interspecific branches (speciation events with Yule diversification) and short intra-specific branches (coalescent processes) (Pons et al., 2006). To test if the ultrametric tree contained both of these branching patterns, the single- and multiple-threshold GMYC models were compared to the null model of one branching process using the SPLITS package v.1.0-19 (Fujisawa and Barraclough, 2013) in R, in which both models had a likelihood ratio test significantly different from the null model ($p = <0.0001$). We also used the Bayesian approach to the GMYC model implemented in the bGMYC R package (Reid and Carstens, 2012), as it incorporates multiple ultrametric trees, thus accounting for phylogenetic uncertainty in tree space, and allows the selection of the posterior probability threshold. There are no specific guidelines for which bGMYC threshold is likely to yield the most accurate results with most authors opting to use a mid-threshold. To ascertain the optimal threshold for our data, we ran a series of analyses setting the

threshold to the lower value of 0.1, and increasing these in increments of 0.1, to the upper threshold of 0.9. A threshold of 0.1 allows for a more conservative approach by reducing the number of false positive results (Musher and Cracraft, 2017), whereas a threshold of 0.9 permits the recovery of potential significant genetic differentiation. The bGMYC algorithm was run for 10000 MCMC generations, sampling every tenth iteration after an initial 500 repetition burn-in. One hundred trees sampled randomly from the posterior distribution of trees were used to perform the analyses as recommended (Reid and Carstens, 2012). We also compared these results to pairwise distances generated for the Cytb sequence data for Africa-Arabian mainland taxa (see Appendix C Table S1). We selected the Kimura-two-parameter (Kimura, 1980) model, implementing the “complete deletion” alignment in MEGA X (Kumar et al., 2018) to ensure comparable sequence lengths (Fregin et al., 2012).

3. Results

3.1 Phylogenetic inference

The Bayesian (Fig. 2) and ML (data not shown) trees generated from the concatenated mtDNA and nuDNA dataset are similar to the mtDNA Bayesian tree (Appendix B, Fig. S1). These hypotheses are generally well-supported (see circled nodes, Fig. 2, Fig. S1), with the exception of the backbone of the tree, which may reflect the rapid diversification of this group. Extensive sampling across sub-Saharan Africa, the southern Arabian Peninsula, western Indian Ocean and Gulf of Guinea regions revealed that as a collective these taxa are monophyletic (hereafter referred to as the Afrotropical radiation, “AR”, Fig. 2), but that this radiation could include the Asian species *Z. palpebrosus*. Although these analyses placed this species as sister to the Afrotropical radiation, this relationship was weakly supported (see also Fig. S1). Despite selecting nuDNA loci based on their utility in previous avian studies investigating recent clades, these data had limited power in resolving relationships of Afrotropical members (Fig. S2). The nuDNA data did, however, provide good support for a clade comprising the subset of Asian taxa sequenced (0.98 BPP), but the position of *Z. palpebrosus*, and the subset of Afrotropical taxa included was unresolved with respect to this clade.

Our results revealed that the Afrotropical *Zosterops* radiation had a complex biogeographical history (Fig. 2) despite the ambiguous position of some clades. We showed that the majority of the western Indian Ocean white-eyes referred to as “Ancient Indian Ocean” (AIO) taxa, *sensu* Warren et al. (2006) - those from Grand Comoro, the Seychelles and the Mascarenes - form a well-supported clade (clade A₁). However, the precise placement of *Z. mouroniensis* (Mount Karthala, Grand Comoro) and the now extinct *Z. semiflavus* (Marianne Island, Seychelles) remains unclear. We also identified a clade composed of the majority of lowland north-east African and southern Arabian forms (grey-bellied birds), including the Socotra island representative of *Z. abyssinicus socotranus* (clade A₂). In the mtDNA only tree, the position of these clades, and taxa, is unresolved with respect to each other, whereas the concatenated tree indicated these groupings may have a close association. Inspection of the nuDNA only data, which included *Z. borbonicus* as a representative of the AIO clade, resolved this taxon as sister to the insular *Z. a. socotranus* (0.86 BPP); however, the relationship between these clades remains to be clarified. In both the concatenated, and mtDNA only trees, these clades A₁ and A₂ are sister to all other Afrotropical members (<50/0.98 BPP respectively). This larger grouping contains the majority of mainland African taxa, including all Gulf of Guinea taxa, and the remaining western Indian Ocean white-eyes, referred to as Indian Ocean ‘*maderaspatanus*’ (IOM), *sensu* Warren et al. (2006).

Afrotropical clade B (0.88 BPP Fig. 2 / 1.00 BPP Fig. S1) is composed solely of mainland taxa, with lowland and highland species interspersed throughout this grouping. Highland taxa (larger, heavier birds) in this clade are from the northern East African sky-islands, while lowland species range from East Africa, through Central Africa (Democratic Republic of Congo) to West Africa (B₁₋₆). The Gulf of Guinea ‘mainland’ (GGM) group, *sensu* Melo et al. (2011) nests within (B₁), and contains morphologically distinctive taxa previously placed in the genus *Speirops*. However, the GGM taxa do not form a strict biogeographic grouping as described by these authors, as *Z. brunnes* (formerly *Speirops brunnes*) forms a clade with *Z. s. stenocricotus* (B₃), but support is only moderate (0.60 BPP) as to its sister group relationship to clade B₄, comprising the East African sky-island taxon *Z. eurycricotus* (Mount Kilimanjaro region) and *Z. melanocephalus* (formerly *Speirops melanocephalus*) from Mount Cameroon.

Afrotropical clade C (1.00 BPP/96% BS, Fig. 2) comprises a further island grouping composed of the remaining western Indian Ocean island endemics - Indian Ocean '*maderaspatanus*' (IOM), *sensu* Warren et al. (2006), denoted as clade C₁, as well as an additional African mainland clade C₂ (Fig. 2). The sister group relationship of the Island of Pemba (East African coast) endemic, *Z. vaughani*, to the IOM clade (C₁) indicates this taxon may have seeded the more distant western Indian Ocean islands of Madagascar, the Comoros and the Seychelles, although support is only moderate for this relationship (0.69 BPP, Fig. 2). The sister group to these western Indian Ocean island birds, is a large clade of mainland taxa (C₂). These include lowland birds from Southern Africa (South Africa, Angola, Mozambique, Zambia, Botswana), but extending into the Democratic Republic of Congo (Kivu region), which are interspersed with the larger, heavier, highland taxa from the southern East African sky-islands.

Finally, a further island clade (D) - Gulf of Guinea 'oceanic' (GGO), *sensu* Melo et al. (2011) - is also identified, concurring with previous phylogenies (Cox et al., 2014; Melo et al., 2011). This clade D is intriguingly resolved as sister to specimens of *Z. abyssinicus socotranus* that originated from the African mainland (northern Somalia), and these taken together are sister to the numerous Afrotropical taxa that comprise clade C. However, in each of these cases the support level is low, so the precise pattern of relationships has yet to be firmly established. It is nevertheless unambiguously clear that, despite their close phenotypic similarity, the mainland population of *Z. abyssinicus socotranus* is only distantly related to that found on the island of Socotra, which are members of clade A₂ (Fig. 2).

3.2 Taxonomy

A major finding of our analysis is that it revealed considerable disagreement with the current taxonomy (van Balen, 2019) as the widespread African mainland taxa *Z. senegalensis sensu lato* and *Z. abyssinicus sensu lato* are non-monophyletic. Our results also supported previous findings (Cox et al., 2014) that showed *Z. poligastrus sensu lato* to be non-monophyletic. However, additional "*poligastrus*" taxa not previously included in that study (*Z. poligastrus sensu stricto*, *Z. kulalensis* and *Z. kaffensis* from northern Kenya and Ethiopia) form a well-supported clade (Fig 2, within clade B₅). We also showed that although many taxa

described as subspecies are monophyletic, this is not the case for all. Along with finding the island (Socotra) and mainland (Somaliland) populations of *Z. abyssinicus socotranus* to be totally unrelated, our results revealed that both *Z. s. senegalensis* and *Z. a. abyssinicus* are also polyphyletic.

3.3 Species delimitation analysis

The bGMYC results implementing 0.1-0.9 thresholds for mainland taxa ranged from 17 to 42 potential species respectively (Table 3). We could reject thresholds of ≤ 0.4 (≤ 21 species) based on taxon lumping that made little biological sense. For example, at this threshold or lower, *Z. senegalensis anderssoni*, *Z. senegalensis stierlingi*, *Z. virens* and *Z. winifredae* were combined, yet the latter two taxa are recognised species based on genetic and phenotypic data (Cox et al., 2014; Habel et al., 2015; Oatley et al., 2017). Similarly, thresholds of ≥ 0.7 (≥ 28 species) were also rejected, as examples of taxon over-splitting occurred. For example, at these thresholds *Z. pallidus* was split, but it is regarded as a diagnosable taxon (Oatley et al., 2011; Oatley et al., 2012), and while it can hybridise with *Z. virens capensis* (Oatley et al., 2017), our samples were selected based on plumages that are consistent with non-hybrids. In this case, the over-splitting appeared to be the result of missing data from the archival samples, which likely introduced longer branch lengths. Although we preferred a threshold of 0.5-0.6 (N=24 mainland species), all thresholds ≥ 0.5 included the likely over split of archival samples of *Z. senegalensis senegalensis* (those in clade B₅, Fig.2) which are from nearby localities (Appendix B). The single and multi-model GYMC recovered 26 and 27 mainland species respectively, but these results may also include examples of over-splitting (see Appendix A for further discussion). Pairwise distances generated from Cyt b also generally support these results (Table S1, Appendix C, and see Appendix A).

Afrotropical radiation island taxa include 17 described species, including the now extinct *Z. semiflavus* (van Balen 2019), which is supported by our findings. However, all thresholds and models clearly showed that the island representative of *Z. a. socotranus* (Socotra white-eye, Appendix A) is a distinct taxon, although this is not well supported based on Cyt b pairwise distances (see Table S1, Appendix C). The western Indian ocean taxa: *Z. maderaspatanus aldabrensis* (Aldabra white-eye) and *Z. maderaspatanus*

comorensis (Moheli white-eye) are also distinct at all thresholds from the nominate *Z. maderaspatanus maderaspatanus* (which groups with the subspecies *Z. m. voeltzkowi* at all thresholds), as well as being non-monophyletic, while *Z. m. anjuanensis* (Anjouan white-eye) is only distinct at thresholds ≥ 0.2 . Lower thresholds ≤ 0.3 (and the single GMYC model) lumped several recognised species together, while higher thresholds ≥ 0.6 (and the GMYC multi-model) split samples of *Z. ficedulinus*. These results indicate a possible 21 island taxa in the region, including *Z. semiflavus*. Our findings are supported in that all Asian species included in the phylogeny were also resolved as independent units. This includes the clustering of *Z. palpebrosus palpebrosus* and *Z. palpebrosus siamensis* (only singletons at a threshold of 0.9), which supports the close affinity of these taxa as noted by Lim et al. (2019). For recommendations regarding a new taxonomy for mainland African white-eyes see Appendix A.

3.4 Molecular divergence dates

As ESS values were initially < 200 for some parameters (including the posterior and prior), we used the HKY model instead of the GTR model (see Table 2B) for the mtDNA data as suggested by BEAST developers. Implementation of this less complex model gave ESS values > 200 in which all runs converged. Our results from this analysis suggested that the Afrotropical realm was colonised very recently from Asia *c.* 1.30 Ma (95% HPD: 1.01-1.61). On colonisation of this realm, there was subsequent rapid divergence (Fig 3), with $\sim 70\%$ of all lineages diverging in the last *c.* 0.5 Ma.

4. Discussion

In this study we generated the first comprehensive species-level phylogeny for Afrotropical Zosteropidae. Our results suggested that the Afrotropics was colonised very recently from Asia at *c.* 1.30 Ma (95% HPD: 1.01-1.61) probably from a single ancestral event. The subsequent rapid colonisation of the Afrotropical realm was however complex, with independent multiple colonisations of both oceanic islands and the ecological sky-islands of the African mainland. Our study also highlighted substantial hidden diversity among mainland taxa, in which the current taxonomic framework greatly underestimated species diversity.

We provide taxonomic recommendations, but highlight that despite harnessing current genetic methodologies white-eyes nevertheless continue to prove a challenging group regarding species delimitation.

4.1 Evolutionary relationships of a “great coloniser”

The exceptional colonisation abilities of *Zosterops* have allowed them to occupy multiple continents and numerous, often remote, oceanic islands, but a lack of detailed sampling has made inferences regarding their evolutionary relationships, and hence colonisation history, difficult to reconcile. Our comprehensive sampling of *Zosterops* taxa from sub-Saharan Africa, the southern Arabian Peninsula, western Indian Ocean and Gulf of Guinea, along with a subset of extra-Afrotropical species, using both archival and fresh material enabled a generally well-supported evaluation of their evolutionary relationships. Despite this, the backbone of the tree proved difficult to resolve, which is unsurprising given the exceptionally rapid diversification of this group (Jetz et al., 2012; Moyle et al., 2009).

We showed that the Afrotropical realm was likely colonised once from Asia, but further investigation is needed as to the position of the lineage comprising the Asian taxa *Z. palpebrosus palpebrosus* and *Z. palpebrosus siamensis*. Although our analyses placed this lineage as sister to the Afrotropical radiation, this was only weakly supported (<50% BPP and BS). A recent study on babblers (Cai et al., 2019), which included 73 described *Zosterops* species, showed that *Z. palpebrosus* grouped with the Ancient Indian Ocean species (*sensu* Warren et al. 2006) and that this clade was sister to all other Afrotropical white-eyes based on their BEAST analysis. If this hypothesis of relationships is correct, the placement of *Z. palpebrosus* within the Afrotropical radiation would indicate a more recent recolonisation of Asia.

We also confirmed that there have been at least two colonisation events of the western Indian Ocean region (AIO and IOM clades, Fig. 2), supporting the findings of Warren et al. (2006), with a further colonisation event of the Gulf of Guinea islands (GGO, Fig. 2), and subsequent radiations within these archipelagos. In addition, single colonisations of the Islands of Socotra, and Pemba have also occurred, highlighting the extraordinary colonisation abilities of *Zosterops* irrespective of descendants being

mainland or island taxa. All previous studies indicated that the AIO group likely occupies a basal position with respect to other Afrotropical members; however, the exact relationships of these members are unclear. While our analyses do not support all Ancient Indian Ocean (AIO) island taxa *sensu* Warren et al. (2006) comprising a clade, support for this arrangement is not strong. Although these taxa were resolved as monophyletic in some previous studies based on mitochondrial loci ND3 + Cytb (Cox et al., 2014; Warren et al., 2006), these taxa were paraphyletic (as indicated in our study) when a larger mtDNA dataset was analysed (Warren et al., 2006). Results from their larger mtDNA dataset also highlighted the instability of the AIO grouping with respect to Asian members, and Cai et al. (2019) found that *Z. palpebrosus* nested within the AIO clade. Clearly the base of the Afrotropical radiation needs further investigation using fast-evolving nuclear loci and additional careful sampling of Asian taxa.

Following colonisation of the Afrotropical realm, there have been subsequent multiple independent colonisations of oceanic islands in the Gulf of Guinea and the western Indian Ocean, and of ecological 'sky-islands' of the African mainland, principally in East Africa. The complex distributions of oceanic island taxa, in which the species from the Gulf of Guinea (Melo et al., 2011) and western Indian Ocean comprise several independent radiations (Melo et al., 2011; Warren et al., 2006), is also mirrored in the complexity of biogeographic relationships of African mainland taxa. Our phylogeny revealed that these mainland taxa cluster within two unrelated clades, in which northern-east Africa sky-island taxa are more closely related to lowland taxa from central and west Africa, whereas southern-east African sky-island taxa are conversely more closely related to lowland taxa from southern African and western central Africa. Cox et al. (2014) showed that each sky-island taxon formerly placed within *Z. poliogastrus sensu lato* and occupying an isolated mountain massif is sister to a lowland species. That study did not include the three most northerly members (*Z. p. poliogastrus*, *Z. kaffensis* and *Z. kulalensis*), recognised as species by van Balen (2019), but which are not supported by any of our species delimitation models (see Appendix A). However, if they are recently diverged species, then this would indicate an example of limited diversification within the highland habitat. We also showed that a further sky-island species - *Z. eurycricotus*, not included in Cox et al. (2014) study, is most closely related to *Z. melanocephalus* from Mount Cameroon in West Africa, and thus

conversely reveals a disjunct relationship between highland species. The ability of *Zosterops* to diversify across large geographic scales is further highlighted in that, whereas the majority of Arabian and north-east African taxa comprise a clade, the novel *Zosterops* sp. nov. from mainland Somalia, which we are in the process of describing and naming, is unrelated to this grouping, nesting much deeper in the tree.

4.2 Timing of colonisation of Afrotropical *Zosterops*

We estimated that the timing of colonisation of the Afrotropics by *Zosterops* occurred relatively recently during the Pleistocene at *c.*1.30 Ma (95% HPD: 1.01-1.61 Ma). This age is in agreement with previous studies that have used the same, or similar island calibrations (Cox, 2013; Moyle et al., 2009; Warren et al., 2006). Although we used similar mtDNA loci to these studies, we included additional nuclear loci (although samples derived from archival DNA do not have these loci sequenced). Moyle et al. (2009) who also used an island calibration, suggested an age of 1.40 – 1.89 Ma for the entire *Zosterops* radiation (two mtDNA loci and one nuclear intron), whereas an earlier age of *c.*3.32 Ma (95% HPD: 2.68-4.15) was generated by the babbler study (Cai et al., 2019), in which the authors used both a geographic and fossil calibration on a larger dataset (12 loci from mt- and nuDNA genomes, although included sequence data for *Zosterops* was incomplete). In the latter study, Afrotropical white-eyes, including the Asian species *Z. palpebrosus*, were estimated to have diverged at *c.*2.16 Ma (95% HPD: 1.80-2.64 Ma), during the Late Pliocene. We acknowledge that the dates generated in our study from a single island calibration are not without uncertainty, as they assume the island taxa evolved in situ (Heads, 2011). This calibration only gives an upper bound of one particular speciation event, and furthermore the calibration also refers to a node that is not well-supported introducing further uncertainty. Our divergence dates should therefore be viewed cautiously, and further investigation is needed to reconcile the ages generated across these different studies. However, a recent study (Leroy et al., 2019) using two independent genomic datasets (mtDNA, and ncDNA), different dating methods, and employing only fossil calibrations to a larger avian tree, indicated diversification for the genus at 1-3.5 Ma, supporting previous studies that have included geological calibrations and a smaller number of loci (although conversely including broader taxon sampling of the

group). Irrespective of calibration used, the colonisation of the Afrotropics by *Zosterops* was clearly a recent one, in which subsequent multiple colonisation events of oceanic and sky-islands islands facilitated their rapid diversification across the entire realm.

4.3 Underestimation of cryptic mainland species

The Africa-Arabia mainland has traditionally been remarkably depauperate in white-eye species, despite the vast size and environmental complexity of this region. Based on the largest genetic assessment of the mainland birds to date we show that the current taxonomic framework greatly underestimates species diversity. In particular, we demonstrated the non-monophyly of the widespread mainland African species “*Z. senegalensis*” *sensu lato* and “*Z. abyssinicus*” *sensu lato*. Previously, Cox et al. (2014) had demonstrated East African montane *Z. poliogastrus sensu lato*, in which they sampled five of the eight subspecies, to be non-monophyletic and suggested these be elevated to species rank; our more comprehensive results support this. That traditional species groupings of *Zosterops* were based largely on plumage colouration (Mees, 1957, 1961, 1969; Moreau, 1957) and, given their rather homogenous appearance, it is not surprising that the taxonomy of the African mainland birds was surrounded by uncertainty and general flux in arrangements (Moreau, 1957). However, despite the seeming failings of plumage coloration regarding species assignment, conversely the majority of subspecies, also defined using this character, have in our phylogeny and subsequent species delimitation analysis been resolved as distinct operational taxonomic units. We suggest that many of these taxa should be elevated to species status rather than remain intraspecific taxa, potentially increasing species diversity of mainland birds, including the Islands of Socotra and Pemba, to 27 species (20 diagnosed species, with a further possible 7 species, which require further study, see Appendix A). Notably, among these species is the extraordinary case of the Socotra white-eye (*Z. socotranus sensu lato*), in which birds formerly classed within the same subspecies (from the Island of Socotra and the northern Somalia mainland) are now shown to be totally unrelated.

Although the use of molecular species delimitation methods provides some clarification to the taxonomy of the group compared to traditional methods based on morphology and plumage (Mees, 1957, 1961, 1969;

Moreau, 1957), there are many instances where results from these analyses are difficult to interpret. While we put forward a provisional revised taxonomy for these mainland birds (see Appendix A) more extensive sampling is required to provide a thorough assessment of species boundaries. We also acknowledge that our analyses of species delimitation has been based on a single locus (i.e. mtDNA), which may not be optimal for species limits (Galtier et al., 2009). For example, issues such as introgression are commonly documented between young species, particularly in areas where there is higher sympatry or parapatry between taxa, as a result of selection, and drift (Ballard and Whitlock, 2004). Hybridisation is a common phenomenon in birds (Ottenburghs et al., 2015), with several studies having documented hybridisation between *Zosterops* subspecies (Milá et al., 2010; Oatley et al., 2017; Oatley et al., 2012), although a recent study of two broadly overlapping young non-sister *Zosterops* species did not show any evidence of past hybridization events (Cowles and Uy, 2019). Although Bayesian implementation of the GMYC has advantages over the original GMYC model, there are also caveats regarding bGMYC and its performance in identifying species that have recently diverged or clades undergoing rapid radiation (Reid and Carstens, 2012), which is likely the case for some of the taxa within this study (see Appendix A). To overcome these limitations additional nuclear genetic data, such as genome-wide RAD-seq, would provide a more powerful resolution of recently evolved species (Ford et al., 2015; Wagner et al., 2013). Ultimately, genetic data should be complemented with other data sets. However, as morphology and ecology may be unreliable for defining species, we suggest behavioural data, such as vocalisation (song) data, could be collected, which has been successfully used to distinguish between several African mainland white-eye species (Husemann et al., 2014). Despite these caveats, the findings of this study should provide a basis for improved conservation assessments of Africa-Arabia mainland birds, since the status of the extremely widespread species previously referred as “*Z. senegalensis*” and “*Z. abyssinicus*” are Least Concern (The IUCN Red List of Threatened Species), yet, many of the newly proposed species occupy considerably more restricted ranges.

Conclusion

Our comprehensive study of Afrotropical zosteropids highlighted substantial hidden species diversity in mainland taxa, likely increasing the already high diversification rate estimated for this group (Moyle et al. 2009), and provided a major update to their taxonomy. Increased diversity of mainland forms was also recently revealed in the widespread Asian species-complex of white-eyes comprising *Z. palpebrosus*, *Z. japonicus* and *Z. montanus* (Lim et al. 2019), indicating that further research is needed into species delimitation, particularly of mainland forms, in one of the world's most iconic 'great speciator' lineages. Future studies will likely require genomic data to disentangle relationships along the backbone of the tree, in which species relationships may ultimately be caused by reticulate evolution, and therefore represented by a network as opposed to a classical bifurcating tree, as revealed in other rapidly radiating lineages (Svardal et al., 2019). Such work will be essential for establishing a robust framework for understanding their evolutionary trajectory and for future conservation assessments. Nevertheless, completion of this comprehensive overview of the phylogenetics of Afrotropical white-eye species provides a major step towards achieving a global synthesis of this fascinating family.

Funding

This work was supported by NERC grant NE/G523612/1 and the Systematics Research Fund. FCM is grateful to the EU's Erasmus Plus program. MI acknowledges support from the Swedish Research Council (grant number 621-2014-5113).

Acknowledgements

We thank Paul Sweet and Tom Trombone, Department of Ornithology, American Museum of Natural History, Jon Fjeldså and Jan Kristensen, Bird Division of Natural History Museum of Denmark and Jan Habel (Technische Universität München) for providing additional samples, and Mark Adams and Hein Van Grouw,

NHM at Tring, for facilitating collection visits. We also thank anonymous reviewers for their helpful comments on an earlier version of this manuscript.

Appendix A. Supplementary material

Taxonomic recommendations, including Plates A-C: Photographs of *Zosterops* specimens from mainland Africa-Arabia and associated islands, including Pemba, Socotra, Gulf of Guinea and the Indian Ocean.

Appendix B. Supplementary material

Table S1. Specimen list, locality data and GenBank accession numbers for molecular sequences used in phylogenetic analyses.

Table S2. Primers used in the amplification of DNA from blood samples.

Table S3. Primers used in the amplification of DNA from archival material.

Appendix C. Supplementary material

Table S1. Pairwise genetic distances for Cytb sequence data using the K2P model.

References

- Ballard, J.W.O., Whitlock, M.C., 2004. The incomplete natural history of mitochondria. *Molecular Ecology*, 729-744.
- Batalha-Filho, H., Pessoa, R.O., Fabre, P.H., Fjeldså, J., Irestedt, M., Ericson, P.G., Silveira, L.F., Miyaki, C.Y., 2014. Phylogeny and historical biogeography of gnateaters (Passeriformes, Conopophagidae) in the South America forests. *Molecular Phylogenetics and Evolution* 79, 422-432.
- Bouckaert, R., Heled, J., Kühnert, D., Vaughan, T., Wu, C.H., Xie, D., Suchard, M.A., A., R., Drummond, A.J., 2014. BEAST 2: A Software Platform for Bayesian Evolutionary Analysis. *PLoS Computational Biology* 10, e1003537.
- Cai, T., Cibois, A., Alström, P., Moyle, R.G., Kennedy, J.D., Shao, S., Zhang, R., Irestedt, M., Per G.P. Ericson, Gelang, M., Qu, Y., Lei, F., Fjeldså, J., 2019. Near-complete phylogeny and taxonomic revision of the world's babblers (Aves: Passeriformes). *Molecular Phylogenetics and Evolution* 130, 346-356.
- Cowles, S.A., Uy, J.A.C., 2019. Rapid, complete reproductive isolation in two closely related *Zosterops* White-eye bird species despite broadly overlapping ranges. *Evolution* 73, 1647-1662.
- Cox, S., 2013. Molecular systematics and diversification of African *Zosteropidae* (Aves: Passeriformes). Department of Genetics, Evolution and Environment. University College London, London.
- Cox, S.C., Prŷs-Jones, R.P., Habel, J.C., Amakobe, B.A., Day, J.J., 2014. Niche divergence promotes rapid diversification of East African sky island white-eyes (Aves: *Zosteropidae*). *Molecular Ecology* 23, 4103-4118.

- Diamond, J.M., Gilpin, M.E., Mayr, E., 1976. Species-distance relation for birds of the Solomon Archipelago, and the paradox of the great speciators. *Proceedings of the National Academy of Sciences, U.S.A.*, 2160-2164.
- Dickinson, E.C., 2003. *The Howard & Moore Complete Checklist of the Birds of the World*. Christopher Helm, London.
- Drummond, A.J., Ho, S.Y., Phillips, M.J., Rambaut, A., 2006. Relaxed phylogenetics and dating with confidence. *PLoS Biology* 4, e88.
- Ford, A.G., Dasmahapatra, K.K., Rüber, L., Gharbi, K., Cezard, T., Day, J.J., 2015. High levels of interspecific gene flow in an endemic cichlid fish adaptive radiation from an extreme lake environment. *Molecular Ecology* 24, 3421-3440.
- Fregin, S., Haase, M., Olsson, U., Alström, P., 2012. Pitfalls in comparisons of genetic distances: A case study of the avian family Acrocephalidae. *Molecular Phylogenetics and Evolution* 62, 319-328.
- Fujisawa, T., Barraclough, T.G., 2013. Delimiting species using single-locus data and the Generalized Mixed Yule Coalescent approach: a revised method and evaluation on simulated data sets. *Systematic Biology* 62, 707-724.
- Galtier, N., Glémin, S., Hurst, G.D.D., 2009. Mitochondrial DNA as a marker of molecular diversity: a reappraisal. *Molecular Ecology* 18, 4541-4550.
- Habel, J.C., Borghesio, L., Newmark, W.D., Day, J.J., Lens, L., Husemann, M., Ulrich, W., 2015. Evolution along the Great Rift Valley: phenotypic and genetic differentiation of East African white-eyes (Aves, Zosteropidae). *Ecology and Evolution* 5, 4849-4862.
- Heads, M., 2011. Old taxa on young islands: a critique of the use of island age to date island-endemic clades and calibrate phylogenies. *Systematic Biology* 60, 204-218.
- Husemann, M., Ulrich, W., Habel, J.C., 2014. The evolution of contact calls in isolated and overlapping populations of two white-eye congeners in East Africa (Aves, *Zosterops*). *BMC Evolutionary Biology* 14, 115.
- Jetz, W., Thomas, G.H., Joy, J.B., Hartmann, K., Mooers, A.O., 2012. The global diversity of birds in space and time. *Nature* 491, 444-448.
- Kearse, M., Moir, R., Wilson, A., Stones-Havas, S., Cheung, M., Sturrock, S., Buxton, S., Cooper, A., Markowitz, S., Duran, C., Thierer, T., Ashton, B., Meintjes, P., Drummond, A., 2012. Geneious Basic: An integrated and extendable desktop software platform for the organization and analysis of sequence data. *Bioinformatics* 28, 1647-1649.
- Kimura, M., 1980. A simple method for estimating evolutionary rates of base substitutions through comparative studies of nucleotide sequences. *Journal of Molecular Evolution* 16, 111-120.
- Kumar, S., Stecher, G., Li, M., Knyaz, C., Tamura, K., 2018. MEGA X: Molecular Evolutionary Genetics Analysis across computing platforms. *Molecular Biology and Evolution* 35, 1547-1549.
- Lanfear, R., Calcott, B., Ho, S.Y.W., Guindon, S., 2012. PartitionFinder: combined selection of partitioning schemes and substitution models for phylogenetic analyses. *Molecular Biology and Evolution* 29, 1695-1701.
- Leroy, T., Anselmetti, Y., Tilak, M.-K., Bérard, S., Csukonyi, L., Gabrielli, G., Scornavacca, C., Milá, B., Thébaud, C., Nabholz, B., 2019. A bird's white-eye view on neoX chromosome evolution. *Peer Community in Evolutionary Biology*.
- Li, Y., Yao, J., Zhao, X., Li, L., Yan, S., 2016. Complete mitochondrial genome sequence of Chestnut-flanked white-eye (*Zosterops erythropleurus*). *Mitochondrial DNA Part A, DNA Mapping Sequencing and Analysis* 27, 3529-3530.
- Lim, B.T.M., Sadanandan, K.R., Dingle, C., Leung, Y.Y., Prawiradilaga, D.M., Irham, M., Ashari, H., Lee, J.G.H., Rheindt, F.E., 2019. Molecular evidence suggests radical revision of species limits in the great speciator white-eye genus *Zosterops*. *Journal of Ornithology* 160, 1-16.
- Mayr, E., 1965. Relationships among Indo-Australian Zosteropidae. *Breviora* 228, 1-6.
- Mees, G.F., 1957. A systematic review of the Indo-Australian Zosteropidae, Part I. *Zoologische Verhandlungen* 35, 1-204.
- Mees, G.F., 1961. A systematic review of the Indo-Australian Zosteropidae, Part II. *Zoologische Verhandlungen* 50, 1-168.

- Mees, G.F., 1969. A systematic review of the Indo-Australian Zosteropidae, Part III. *Zoologische Verhandelingen* 102, 1-390.
- Melo, M., Warren, B.H., Jones, P.J., 2011. Rapid parallel evolution of aberrant traits in the diversification of the Gulf of Guinea white-eye (Aves, Zosteropidae). *Molecular Ecology* 20, 4953-4967.
- Milá, B., Warren, B.H., Heeb, P., Thébaud, C., 2010. The geographic scale of diversification on islands: genetic and morphological divergence at a very small spatial scale in the Mascarene grey white-eye (Aves: *Zosterops borbonicus*). *BMC Evolutionary Biology* 10, 158-171.
- Miller, M.A., Pfeiffer, W., Schwartz, T., 2010. Creating the CIPRES Science Gateway for inference of large phylogenetic trees. *Proceedings of the Gateway Computing Environments Workshop (GCE)*, 1 - 8.
- Moreau, R.E., 1957. Variation in the western Zosteropidae (Aves). *Bulletin of the British Museum* 4, 318-433.
- Moreau, R.E., 1967. Family Zosteropidae, white-eyes: African and Indian Ocean taxa. In: Paynter, R.A., Mayr, E. (Eds.), *Check-list of the birds of the world*. Museum of Comparative Zoology Cambridge, M.A. USA, pp. 326-337.
- Moyle, R.G., Andersen, M.J., Oliveros, C.H., Steinheimer, F., Reddy, S., 2012. Phylogeny and biogeography of the core babblers (Aves: Timaliidae). *Systematic Biology* 61, 631-651.
- Moyle, R.G., Filardi, C.E., Smith, C.E., Diamond, J.C., 2009. Explosive pleistocene diversification and hemispheric expansion of a “great speciator”. *Proceedings of the National Academy of Sciences, U.S.A.* 106, 1863–1868.
- Mundy, N.I., Unitt, P., Woodruff, D.S., 1997. Skin from feet of museum specimens as a non-destructive source of DNA for Avian genotyping. *The Auk* 114, 126-129.
- Musher, I., Cracraft, J., 2017. Phylogenomics and species delimitation of a complex radiation of Neotropical suboscine birds (*Pachyramphus*). *Molecular Phylogenetics and Evolution* 118, 204-221.
- Oatley, G., Bowie, R.C.K., Crowe, T.M., 2011. The use of subspecies in the systematics of southern African white-eyes: historical entities or eco-geographic variants *Journal of Zoology* 284, 21-30.
- Oatley, G., De Swardt, D.H., Nuttall, R.J., Crowe, T.M., Bowie, R.C.K., 2017. Phenotypic and genotypic variation across a stable white-eye (*Zosterops* sp.) hybrid zone in central South Africa. *Biological Journal of the Linnean Society* 121, 670-684.
- Oatley, G., Voelker, G., Crowe, T.M., Bowie, R.C.K., 2012. A multi-locus phylogeny reveals a complex pattern of diversification related to climate and habitat heterogeneity in southern African white-eyes. *Molecular Phylogenetics and Evolution* 64, 633-644.
- Ottenburghs, J., Ydenberg, C.R., Van Hooft, P., Van Wieren, S.E., Prins, H.H., 2015. The Avian Hybrids Project: gathering the scientific literature on avian hybridization. *Ibis* 157, 892-894.
- Paradis, E., Claude, J., Strimmer, K., 2004. APE: Analyses of Phylogenetics and Evolution in R language. *Bioinformatics* 20, 289-290.
- Pearson, D.J., Turner, D.A., 2017. A taxonomic review of the genus *Zosterops* in East Africa, with a revised list of species occurring in Kenya, Uganda and Tanzania. *Scopus* 37, 1-13.
- Phillimore, A.B., Owens, I.P.F., Black, R.A., Chittock, J., Burke, T., Clegg, S.M., 2008. Complex patterns of genetic and phenotypic divergence in an island bird and the consequences for delimiting conservation units. *Molecular Ecology* 17, 2839-2853.
- Pons, J., Barraclough, T.G., Gomez-Zurita, J., Cardoso, A., Duran, D.P., Hazell, S., Kamoun, S., Sumlin, W.D., Vogler, A.P., 2006. Sequence-based species delimitation for the DNA taxonomy of undescribed insects. *Systematic Biology* 55, 595-609.
- Powell, J.R., 2012. Accounting for uncertainty in species delineation during the analysis of environmental DNA sequence data. *Methods in Ecology and Evolution* 3, 1-11.
- R Development Core Team, 2018. R: A Language and Environment for Statistical Computing. R Foundation for Statistical Computing. Vienna, <http://www.R-project.org/>.
- Rambaut, A., Drummond, A.J., Xie, D., Baele, G., Suchard, M.A., 2018. Posterior summarisation in Bayesian phylogenetics using Tracer 1.7. *Systematic Biology* 67, 901-904.
- Reid, N.M., Carstens, B.C., 2012. Phylogenetic estimation error can decrease the accuracy of species delimitation: a Bayesian implementation of the general mixed Yule-coalescent model. *BMC Evolutionary Biology* 12, 196.

- Rocha, T.C., Sequeira, F., Aleixo, A., Rego, P.S., Sampaio, I., Schneider, H., Vallinoto, M., 2015. Molecular phylogeny and diversification of a widespread Neotropical rainforest bird group: The Buff-throated Woodcreeper complex, *Xiphorhynchus guttatus/susurrans* (Aves: Dendrocolaptidae). *Molecular Phylogenetics and Evolution* 85, 131-140.
- Ronquist, F., Huelsenbeck, J.P., 2003. MRBAYES 3: Bayesian phylogenetic inference under mixed models. *Bioinformatics* 19, 1572-1574.
- Slikas, B., Jones, I.B., Derrickson, S.R., Fleischer, R.C., 2000. Phylogenetic relationships of Micronesian White-eyes based on mitochondrial sequence data. *The Auk* 117, 355-365.
- Sukumaran, J., Holder, M.T., 2010. DendroPy: a Python library for phylogenetic computing. *Bioinformatics* 26, 1569-1571.
- Svardal, H., Quah, F.X., Malinsky, M., Ngatunga, B.P., Miska, E.A., Salzburger, W., Genner, M.J., Turner, G.F., Durbin, R., 2019. Ancestral Hybridization Facilitated Species Diversification in the Lake Malawi Cichlid Fish Adaptive Radiation, *Molecular Biology and Evolution*, *Molecular Biology and Evolution*.
- Swofford, D., 2002. PAUP*: phylogenetic analysis using parsimony (* and other methods). Sunderland, MA.
- The IUCN Red List of Threatened Species, 2018. Version 2018-1. <www.iucnredlist.org>. Downloaded on 11 September 2018.
- van Balen, B., 2019. White-eyes and Yuhinas (Zosteropidae). In: del Hoyo, J., Elliott, A., Sargatal, J., Christie, D.A., de Juana, E. (Eds.), *Handbook of the Birds of the World Alive*. Lynx Edicions, Barcelona. (retrieved from <https://www.hbw.com/node/52351> on 15 September 2019).
- Wagner, C.E., Keller, I., Wittwer, S., Selz, O.M., Mwaiko, S., Greuter, L., Sivasundar, A., Seehausen, O., 2013. Genome-wide RAD sequence data provide unprecedented resolution of species boundaries and relationships in the Lake Victoria cichlid adaptive radiation. *Molecular Ecology* 22, 787-798.
- Warren, B., Bermingham, E., Prŷs-Jones, R.P., Thebauds, C., 2006. Immigration, species radiation and extinction in a highly diverse songbird lineage: white-eyes on the Indian Ocean islands. *Molecular Ecology* 15, 3769-3786.
- Zuccon, D., Ericson, P.G., 2012. Molecular and morphological evidences place the extinct New Zealand endemic *Turnagra capensis* in the Oriolidae. *Molecular Phylogenetics and Evolution* 62, 414-426.
- Zwickl, D.J., 2006. Genetic algorithm approaches for the phylogenetic analysis of large biological sequence datasets under the maximum likelihood criterion. The University of Texas, Austin.

Table 2. The optimal partitioning schemes as generated by PartitionFinder v.2.11 for nucleotide data using the Bayesian information criterion (BIC) for a) Mr Bayes, GARLI and BEAST analyses including 161 samples; b) BEAST analysis based on 57 taxa.

A.

Locus	Best fitting model
ND3 codon 1	HKI+I+G
ATP6 codon 2	
ND3 codon 2	HKY+I+G
ATP6 codon 1	TrN+I+G
ND3 codon 3	
Cytb codon 1	K81+I+G
ATP codon 3	HKI+I
Cyt b codon 2	
Cyt b codon 3	TrN+G
TGF β 2	
G3PDH	
FIB7	HKI+I
CHD1	
MUSK	

B.

Locus	Best fitting model
ND3	GTR+I+G
Cyt b	
ATPase6	
TGF β 2	K80+I
G3PDH	
FIB7	HKY+I
CHD1	
MUSK	

Table 3. Species delimitation of Afrotropical mainland and island birds based on bGMYC (thresholds 0.1-0.9) and GMYC (single- and multi-models), including extra-Afrotropical taxa (included within the phylogeny) for comparative purposes. Grey boxes for extra-Afrotropical taxa correspond to the number of described species (van Balen 2019), while grey boxes for the Afrotropical taxa (mainland and island) represent the preferred thresholds (see Appendix A for discussion).

Threshold or model	bGMYC									GMYC	
	0.1	0.2	0.3	0.4	0.5	0.6	0.7	0.8	0.9	Single	Multi
Mainland	17	19	20	21	24	24	28	34	42	26	27
Island	16	19	20	21	21	22	22	22	22	20	22
Extra-Afrotropical	10	10	10	10	10	10	10	10	11	11	10

Figure 1. A) Global distribution of samples; and B) Afrotropical distribution of samples, including Africa-Arabia and associated Western Indian Ocean and Gulf of Guinea Islands, included in the phylogeny. Colours refer to the traditional taxonomy (Dickinson, 2003) for “*Z. abyssinicus*” *sensu lato* (green), “*Z. senegalensis*” *sensu lato* (yellow), and “*Z. poligastrus*” *sensu lato* (red); Island taxa (apart from Socotra and Pemba) within the Afrotropical radiation (grey); extra-Afrotropical taxa (black). Ranges are from The IUCN Red List of Threatened Species (2018).

Figure 2. Phylogeny of Afrotropical *Zosterops* from Sub-Saharan Africa, the Arabian Peninsula, Gulf of Aden, Gulf of Guinea and western Indian Ocean islands, and including a subset of Asian taxa. This tree is generated using Bayesian inference from all loci (mtDNA and nuDNA). Taxon names to the right are based on the current taxonomy of van Balen (2019), with names to the left based on our revised taxonomy (see Appendix A) if different. Included taxonomic symbols: squares = mainland taxa; triangles = island taxa; white = western Indian Ocean taxa; grey = Gulf of Guinea taxa; red = “*Z. poligastrus*” *sensu lato*; yellow = “*Z. senegalensis*” *sensu lato*; green = “*Z. abyssinicus*” *sensu lato*; colours refer to the traditional taxonomy of Dickinson (2003). Side-bar: grey boxes = island taxa; white boxes = lowland mainland taxa; black boxes = upland mainland taxa. Outgroup taxa (Asia-Pacific) denoted by white box. Support: below branches = Bayesian Posterior Probabilities (BPP), above branches = bootstrap (bs).

Figure 3. Time tree of Afrotropical *Zosterops*, including Asian outgroups and the more distant outgroup *Zosterornis whiteheadi*. Taxon names follow the proposed taxonomy (Appendix A). Calibration denoted by a black bar; blue bars represent 95% HPDs (for details of calibration see section 2.4). Included symbols: squares = mainland taxa; triangles = island taxa; white = western Indian Ocean taxa; grey = Gulf of Guinea taxa; red = “*Z. poligastrus*” *sensu lato*; yellow = “*Z. senegalensis*” *sensu lato*; green = “*Z. abyssinicus*” *sensu lato*; colours refer to the traditional taxonomy of Dickinson (2003). Filled grey box includes outgroup taxa (extra-Afrotropical).

van Balen (2019)	Proposed taxonomy (if different)	Country	Locality	Lat.	Long.	Voucher/ Field no.
<i>Z. abyssinicus abyssinicus</i>	<i>Z. abyssinicus</i>	Eritrea	Ghinda	15.378	39.093	BMNH 1951.55.1
<i>Z. abyssinicus abyssinicus</i>	<i>Z. abyssinicus</i>	Eritrea	Ghinda	15.378	39.093	BMNH 1951.55.2
<i>Z. abyssinicus abyssinicus</i>	<i>Z. abyssinicus</i>	Ethiopia	South Gondar	11.693	37.532	BMNH 1927.11.5.554
<i>Z. abyssinicus abyssinicus</i>	<i>Z. abyssinicus</i>	Ethiopia	South Gondar	11.693	37.532	BMNH 1927.11.5.578
<i>Z. abyssinicus abyssinicus</i>	<i>Z. abyssinicus</i>	Sudan	Port Sudan	18.633	36.970	BMNH 1919.12.17.1048
<i>Z. abyssinicus arabs</i>	<i>Z. abyssinicus</i>	Saudi Arabia	Taif	21.294	40.358	BMNH 1935.5.10.48
<i>Z. abyssinicus arabs</i>	<i>Z. abyssinicus</i>	Yemen	Menacha,	15.074	43.733	BMNH 1913.7.18.44
<i>Z. abyssinicus omoensis</i>	<i>Z. abyssinicus</i>	Ethiopia	Lake Turkana	4.767	35.992	BMNH 1912.10.15.1275
<i>Z. abyssinicus omoensis</i>	<i>Z. abyssinicus</i>	Ethiopia	Gofa	6.250	36.750	BMNH 1912.10.15.1920
<i>Z. abyssinicus omoensis</i>	<i>Z. abyssinicus</i>	Ethiopia	Lake Tana	11.967	36.962	BMNH 1927.11.5.580
<i>Z. abyssinicus socotranus</i>	<i>Z. socotranus</i>	Yemen	Socotra Island	12.500	54.000	BW293
<i>Z. abyssinicus socotranus</i>	<i>Z. socotranus</i>	Yemen	Socotra Island	12.633	54.000	BMNH 1953.36.34
<i>Z. abyssinicus socotranus</i>	<i>Z. socotranus</i>	Yemen	Socotra Island	12.555	54.073	BMNH 1934.8.12.23
<i>Z. abyssinicus socotranus</i>	<i>Z. sp. nov.</i>	Somalia	Sanaag	10.969	48.749	BMNH 1923.8.7.2987
<i>Z. abyssinicus socotranus</i>	<i>Z. sp. nov.</i>	Somalia	Sanaag	10.969	48.749	BMNH 1923.8.7.2990
<i>Z. abyssinicus socotranus</i>	<i>Z. sp. nov.</i>	Somalia	Sanaag	10.969	48.749	BMNH 1923.8.7.2989
<i>Z. abyssinicus socotranus</i>	<i>Z. sp. nov.</i>	Somalia	Sanaag	10.969	48.749	BMNH 1923.8.7.2996
<i>Z. atricapilla</i>		Borneo	Mt Trusmadi,Sabah	5.563	116.494	LSUMNS B36434
<i>Z. atricapilla</i>		Borneo	Mt Trusmadi,Sabah	5.563	116.494	LSUMNS B36444
<i>Z. atrifrons</i>		Indonesia	Poso	-1.521	120.419	AMNH DOT12589
<i>Z. atrifrons</i>		Indonesia	Banggai	-0.736	123.002	AMNH DOT12620
<i>Z. borbonicus</i>		Mascarens	La Reunion	-21.104	55.420	BWM46
<i>Z. borbonicus</i>		Mascarens	La Reunion	-21.104	55.420	BWM54
<i>Z. brunneus</i>		Equatorial Guinea	Bioko	3.574	8.693	MM BRU001
<i>Z. brunneus</i>		Equatorial Guinea	Bioko	3.574	8.693	MM BRU003
<i>Z. chloronothos</i>		Mascarens	Mauritius	-20.318	57.506	BWM28
<i>Z. chloronothos</i>		Mascarens	Mauritius	-20.318	57.506	BWM29
<i>Z. erythropleurus</i>		China	Tianjin	40.461	117.237	KT194322
<i>Z. erythropleurus</i>		China	Baidaihe, Hebei	39.822	119.454	ZMUC O2653
<i>Z. eurycricotus</i>		Tanzania	Simba Forest	-3.200	35.467	ZMUC 121003
<i>Z. eurycricotus</i>		Tanzania	Simba Forest	-3.200	35.467	ZMUC 121004
<i>Z. eurycricotus</i>		Tanzania	Mt Meru	-3.233	36.750	NRM 570798

<i>Z. euryricotus</i>		Tanzania	Mt Meru	-3.233	36.750	NRM 570799
<i>Z. feae</i>		São Tomé and Príncipe	São Tomé Island	0.246	6.594	MM FIS002
<i>Z. feae</i>		São Tomé and Príncipe	São Tomé Island	0.246	6.594	MM FIS003
<i>Z. ficedulinus</i>		Equatorial Guinea	Principe Island	-1.435	5.626	MM FIP001
<i>Z. ficedulinus</i>		Equatorial Guinea	Principe Island	-1.435	5.626	MM FIP002
<i>Z. flavilateralis flavilateralis</i>	<i>Z. flavilateralis</i>	Kenya	Umani spring	-2.467	37.914	COX T4
<i>Z. flavilateralis flavilateralis</i>	<i>Z. flavilateralis</i>	Kenya	Umani spring	-2.467	37.914	COX T15
<i>Z. flavilateralis flavilateralis</i>	<i>Z. flavilateralis</i>	Kenya	Umani spring	-2.467	37.914	COX T21
<i>Z. flavilateralis jubaensis</i>	<i>Z. flavilateralis</i>	Kenya	South Horr	2.106	36.880	COX T69
<i>Z. flavilateralis jubaensis</i>	<i>Z. flavilateralis</i>	Kenya	South Horr	2.106	36.880	COX T70
<i>Z. flavilateralis jubaensis</i>	<i>Z. flavilateralis</i>	Kenya	South Horr	2.106	36.880	COX T77
<i>Z. griseovirescens</i>		São Tomé and Príncipe	Annobon	1.590	7.375	MM GRI001
<i>Z. griseovirescens</i>		São Tomé and Príncipe	Annobon	1.590	7.375	MM GRI002
<i>Z. hypoxanthus</i>		Papua New Guinea	New Irland	-3.367	152.005	AMNH DOT20050
<i>Z. hypoxanthus</i>		Papua New Guinea	New Irland	-3.367	152.005	AMNH DOT20052
<i>Z. kaffensis</i>	<i>Z. poligastus</i>	Ethiopia	Jimma, Ethiopia	7.667	36.833	BMNH 1912.10.15.1932
<i>Z. kaffensis</i>	<i>Z. poligastus</i>	Ethiopia	Charada forest	7.350	36.450	BMNH 1912.10.15.1262
<i>Z. kikuyuensis</i>		Kenya	Aberdares Range	-0.385	36.636	JH AB12
<i>Z. kikuyuensis</i>		Kenya	Aberdares Range	-0.385	36.636	JH AB20
<i>Z. kikuyuensis</i>		Kenya	Aberdares Range	-0.385	36.636	JH AB4
<i>Z. kirki</i>		Comoros	Grande Comore	-11.775	43.334	BW146
<i>Z. kirki</i>		Comoros	Grande Comore	-11.775	43.334	BW147
<i>Z. kulalensis</i>	<i>Z. poligastus</i>	Kenya	Mt Kulal	2.733	36.938	COX K30
<i>Z. kulalensis</i>	<i>Z. poligastus</i>	Kenya	Mt Kulal	2.733	36.938	COX K33
<i>Z. kulalensis</i>	<i>Z. poligastus</i>	Kenya	Mt Kulal	2.733	36.938	JH 2MK7
<i>Z. lateralis chloronotus</i>		Australia	Ravensthorpe	-33.764	119.827	AMNH DOT17779
<i>Z. lateralis chloronotus</i>		Australia	Ravensthorpe	-33.764	119.827	AMNH DOT17785
<i>Z. leucophaeus</i>		São Tomé and Príncipe	Principe	1.590	7.375	MM LEU001
<i>Z. leucophaeus</i>		São Tomé and Príncipe	Principe	1.590	7.375	MM LEU002
<i>Z. lugubris</i>		São Tomé and Príncipe	Sao Tome	0.246	6.594	MM LUG011
<i>Z. lugubris</i>		São Tomé and Príncipe	Sao Tome	0.246	6.594	MM2
<i>Z. maderaspatanus aldabrensis</i>		Seychelles	Aldabra	-9.416	46.390	BW301
<i>Z. maderaspatanus aldabrensis</i>		Seychelles	Aldabra	-9.416	46.390	BW303
<i>Z. maderaspatanus anjuanensis</i>		Comoros	Anjuan	-12.219	44.414	BW252

<i>Z. maderaspatanus anjuanensis</i>		Comoros	Anjouan	-12.219	44.414	BW253
<i>Z. maderaspatanus comorensis</i>		Comoros	Moheli	-12.336	43.703	BW121
<i>Z. maderaspatanus comorensis</i>		Comoros	Moheli	-12.336	43.703	BW127
<i>Z. maderaspatanus maderaspatanus</i>		Madagascar	Mt Ankaratre	-19.360	47.300	BW429
<i>Z. maderaspatanus maderaspatanus</i>		Madagascar	Mt Ankaratre	-19.360	47.300	BW445
<i>Z. maderaspatanus voeltzkowi</i>		France	Europa Island	-22.341	40.347	BW ML26
<i>Z. maderaspatanus voeltzkowi</i>		France	Europa Island	-22.341	40.347	BW ML30
<i>Z. mauritanus</i>		Mascarens	Mauritus	-20.280	57.436	BWM17
<i>Z. mauritanus</i>		Mascarens	Mauritus	-20.280	57.436	BWM24
<i>Z. mayottensis</i>		France	Mayotte Island	-12.834	45.126	BW64
<i>Z. mayottensis</i>		France	Mayotte Island	-12.834	45.126	BW67
<i>Z. mbuluensis</i>		Kenya	Chyulu Hills	-2.547	37.812	JH CH7
<i>Z. mbuluensis</i>		Kenya	Chyulu Hills	-2.547	37.812	JH CH8
<i>Z. mbuluensis</i>		Kenya	Chyulu Hills	-2.547	37.812	JH 2CH11
<i>Z. melanocephalus</i>		Cameroon	Mt Cameroon	4.217	9.074	MM MEL002
<i>Z. melanocephalus</i>		Cameroon	Mt Cameroon	4.217	9.074	MM MEL001
<i>Z. modestus</i>		Seychelles	Conception	-4.663	55.364	BW344
<i>Z. modestus</i>		Seychelles	Conception	-4.663	55.364	BW345
<i>Z. montanus whiteheadi</i>		Philippines	Mt Pilog, Luzon	16.602	120.900	ZMUC O2655
<i>Z. montanus whiteheadi</i>		Philippines	Mt Pilog, Luzon	16.602	120.900	ZMUC O2662
<i>Z. mouroniensis</i>		Comoros	Grande Comore	-11.775	43.334	BW137
<i>Z. mouroniensis</i>		Comoros	Grande Comore	-11.775	43.334	BW140
<i>Z. nigrorum</i>		Philippines		16.447	121.224	FMNH 432997
<i>Z. nigrorum aureiloris</i>		Philippines	Dinapigue, Isabella	16.693	122.231	ZMUC O2663
<i>Z. olivaceus</i>		Mascarens	La Reunion	-21.101	55.436	BWM49
<i>Z. olivaceus</i>		Mascarens	La Reunion	-21.101	55.436	BWM55
<i>Z. pallidus</i>		South Africa		-28.705	17.364	PFAO AP50340
<i>Z. pallidus</i>		Namibia	Great Namaqualand	-26.780	17.800	BMNH 1950.50.666
<i>Z. pallidus</i>		South Africa	Venterskroon	-26.900	27.267	BMNH 1928.2.2.12
<i>Z. pallidus</i>		South Africa	Fourteen Streams	-28.080	24.896	BMNH 1904.11.19.56
<i>Z. pallidus</i>		South Africa	Bloemfontein	-29.121	26.214	BMNH 1923.8.7.2982
<i>Z. palpebrosus palpebrosus</i>		Nepal	Betrawati	27.975	85.208	AMNH DOT5746
<i>Z. palpebrosus palpebrosus</i>		Nepal	Betrawati	27.975	85.208	RF1
<i>Z. palpebrosus siamensis</i>		Vietnam	Ha Giang	22.754	104.827	AMNH DOT6512

<i>Z. palpebrosus siamensis</i>		Vietnam	Ha Giang	22.754	104.827	AMNH DOT2659
<i>Z. aff. poligastrus (sensu lato)</i>	<i>Z. poligastrus</i>	Ethiopia	Fetche	7.738	36.716	JH FS79
<i>Z. aff. poligastrus (sensu lato)</i>	<i>Z. poligastrus</i>	Ethiopia	Garuke	7.730	36.980	JH FS95
<i>Z. aff. poligastrus (sensu lato)</i>	<i>Z. poligastrus</i>	Ethiopia	Gera	7.531	36.378	JH FS43
<i>Z. poligastrus</i>	<i>Z. poligastrus</i>	Eritrea	Faghena	15.583	38.876	BMNH 1954.24.21
<i>Z. poligastrus</i>	<i>Z. poligastrus</i>	Ethiopia	Borena	10.750	38.767	BMNH 1946.5.2433
<i>Z. semiflavus</i>		Seychelles	Marianne Island	-4.341	55.918	BMNH 1927.12.18.398
<i>Z. senegalensis anderssoni</i>	<i>Z. anderssoni</i>	Botswana	Kasane	-17.816	25.131	BMNH 1932.5.5.126
<i>Z. senegalensis anderssoni</i>	<i>Z. anderssoni</i>	Mozambique	Mount Namuli	-15.374	37.041	BMNH 2008.10.33
<i>Z. senegalensis anderssoni</i>	<i>Z. anderssoni</i>	Mozambique	Mount Namuli	-15.374	37.041	BMNH 2008.10.32
<i>Z. senegalensis anderssoni</i>	<i>Z. anderssoni</i>	Zambia	Livingstone	-17.891	25.830	BMNH 1947.75.10
<i>Z. senegalensis anderssoni</i>	<i>Z. anderssoni</i>	DRC		-10.796	27.027	BMNH 1936.4.13.66
<i>Z. senegalensis anderssoni</i>	<i>Z. anderssoni</i>	DRC		-10.796	27.027	BMNH 1936.4.13.65
<i>Z. senegalensis senegalensis</i>	<i>Z. senegalensis</i>	Ghana	Kintampo	8.056	-1.731	BMNH 1911.12.23.2612
<i>Z. senegalensis demeryi</i>	<i>Z. senegalensis</i>	Liberia	Mt Nimba	7.489	-8.571	BMNH 1977.20.2492
<i>Z. senegalensis gerhardi</i>	<i>Z. jacksoni</i>	South Sudan	Didinga Hills	4.334	33.581	BMNH 1939.10.1.284
<i>Z. senegalensis heinrichi</i>	<i>Z. quanzae</i>	Angola	N'dalatando	-9.301	14.877	BMNH 1910.5.6.1047
<i>Z. senegalensis heinrichi</i>	<i>Z. quanzae</i>	Angola	N'dalatando	-9.301	14.877	BMNH 1910.5.6.1052
<i>Z. senegalensis heinrichi</i>	<i>Z. quanzae</i>	Angola	Luena	-11.780	19.870	BMNH 1957.35.527
<i>Z. senegalensis jacksoni</i>	<i>Z. jacksoni</i>	Kenya	Mt Nyiru	2.133	36.850	BLS35
<i>Z. senegalensis jacksoni</i>	<i>Z. jacksoni</i>	Kenya	Mathews Range	1.282	37.298	BLS77
<i>Z. senegalensis jacksoni</i>	<i>Z. jacksoni</i>	Kenya	Aberdares Range	1.050	36.850	ZMUC 146784
<i>Z. senegalensis kasaicus</i>	<i>Z. quanzae</i>	Angola	N'dalatando	-9.280	14.901	BMNH 1910.5.6.1049
<i>Z. senegalensis quanzae</i>	<i>Z. quanzae</i>	Angola	Quipeia	-10.574	15.862	BMNH 1957.35.331
<i>Z. senegalensis quanzae</i>	<i>Z. quanzae</i>	Angola	Quipeia	-10.574	15.862	BMNH1957.35.530
<i>Z. senegalensis reichenowi</i>		Uganda	Mubuku Valley	0.269	30.103	BMNH 1906.12.23.718
<i>Z. senegalensis senegalensis</i>	<i>Z. senegalensis</i>	Liberia	Mt Nimba	7.535	-8.517	BMNH 1977.20.2495
<i>Z. senegalensis senegalensis</i>	<i>Z. senegalensis</i>	Nigeria	Tunga	8.160	7.500	BMNH 1938.8.3.10
<i>Z. senegalensis senegalensis</i>	<i>Z. stuhlmanni</i>	Uganda	Mt Rwenzori	0.241	29.876	ZMUC 145103
<i>Z. senegalensis senegalensis</i>	<i>Z. stuhlmanni</i>	Uganda	Mt Rwenzori	0.241	29.876	ZMUC 145211
<i>Z. senegalensis senegalensis</i>	<i>Z. stuhlmanni</i>	DRC	Kivu	-2.249	28.835	ZMUC 128660
<i>Z. senegalensis senegalensis</i>	<i>Z. stuhlmanni</i>	DRC	Kivu	-2.249	28.835	ZMUC 128658
<i>Z. senegalensis senegalensis</i>	<i>Z. senegalensis</i>	Ghana		9.308	-1.244	LSUMZ B39250
<i>Z. senegalensis senegalensis</i>	<i>Z. senegalensis</i>	Ghana		10.710	-0.555	LSUMZ B39514

<i>Z. senegalensis stenocricotus</i>	<i>Z. stenocricotus</i>	Cameroon	Mt Cameroon	4.170	9.200	BMNH 1966.16.3386
<i>Z. senegalensis stenocricotus</i>	<i>Z. stenocricotus</i>	Cameroon	Mt Cameroon	4.170	9.200	MM STC01
<i>Z. senegalensis stenocricotus</i>	<i>Z. stenocricotus</i>	Equatorial Guinea	Bioko	3.573	8.692	MM STB001
<i>Z. senegalensis stenocricotus</i>	<i>Z. stenocricotus</i>	Equatorial Guinea	Bioko	3.573	8.692	MM STB002
<i>Z. senegalensis stierlingi</i>	<i>Z. anderssoni</i>	Tanzania	Ndundulu Mts	-7.800	36.500	ZMUC 118724
<i>Z. senegalensis stierlingi</i>	<i>Z. anderssoni</i>	Tanzania	Ndundulu Mts	-7.800	36.500	ZMUC 118792
<i>Z. senegalensis stierlingi</i>	<i>Z. anderssoni</i>	Tanzania	Poroto Mts	-9.017	33.750	ZMUC 142607
<i>Z. senegalensis stuhlmanni</i>	<i>Z. stuhlmanni</i>	Uganda	Mpumuru	0.517	30.317	BMNH 1913.7.16.140
<i>Z. senegalensis stuhlmanni</i>	<i>Z. stuhlmanni</i>	Uganda	Entebbe	0.075	32.472	BMNH 1906.12.11.80
<i>Z. senegalensis tongensis</i>	<i>Z. anderssoni</i>	Mozambique	Coguno	-24.390	34.553	BMNH 1905.12.29.1713
<i>Z. senegalensis toroensis</i>		DRC	Godema	1.978	30.697	BMNH 1936.2.21.237
<i>Z. silvanus</i>		Kenya	Taita Hills	-3.383	38.361	JH TH13
<i>Z. silvanus</i>		Kenya	Taita Hills	-3.383	38.361	JH TH212
<i>Z. silvanus</i>		Kenya	Taita Hills	-3.383	38.361	JH TH215
<i>Z. splendidus</i>		Solomon Islands	Ranongga Isl	-8.061	156.562	AMNH DOT171
<i>Z. splendidus</i>		Solomon Islands	Ranongga Isl	-8.061	156.562	AMNH DOT174
<i>Z. vaughani</i>		Tanzania	Pemba Island	-4.948	39.676	BMNH 1947.5.41
<i>Z. vaughani</i>		Tanzania	Pemba Island	-4.948	39.676	BMNH 1947.5.53
<i>Z. virens capensis</i>	<i>Z. virens</i>	South Africa	Knysna	-34.083	23.067	BMNH 1905.12.29.1741
<i>Z. virens capensis</i>	<i>Z. virens</i>	South Africa	Cape Town	-33.960	18.409	PFIAO K1
<i>Z. virens virens</i>	<i>Z. virens</i>	South Africa		-26.075	29.262	PFIAO AM36426
<i>Z. virens virens</i>	<i>Z. virens</i>	South Africa		-26.075	29.262	PFIAO AM36429
<i>Z. virens virens</i>	<i>Z. virens</i>	South Africa		-26.075	29.262	PFIAO AM36433
<i>Z. winnifredae</i>		Tanzania	Mount Shengena	-4.311	37.933	ZMUC 121694
<i>Z. winnifredae</i>		Tanzania	Mount Shengena	-4.311	37.933	ZMUC 121698
<i>Z. winnifredae</i>		Tanzania	S. Pare Mts	-4.045	37.735	ZMUC O5899
<i>Zosterornis whiteheadi</i>		Philippines		13.909	122.959	KUNHM 18001

Journal Pre-proofs

Table 2. The optimal partitioning schemes as generated by PartitionFinder v.2.11 for nucleotide data using the Bayesian information criterion (BIC) for a) Mr Bayes, GARLI and BEAST analyses including 161 samples; b) BEAST analysis based on 57 taxa.

A.

Locus	Best fitting model
ND3 codon 1	HKI+I+G
ATP6 codon 2	
ND3 codon 2	HKY+I+G
ATP6 codon 1	TrN+I+G
ND3 codon 3	
Cytb codon 1	K81+I+G
ATP codon 3	HKI+I
Cyt b codon 2	
Cyt b codon 3	TrN+G
TGF β 2	
G3PDH	
FIB7	HKI+I
CHD1	
MUSK	

B.

Locus	Best fitting model
ND3	GTR+I+G
Cyt b	
ATPase6	
TGF β 2	K80+I
G3PDH	
FIB7	HKY+I
CHD1	
MUSK	

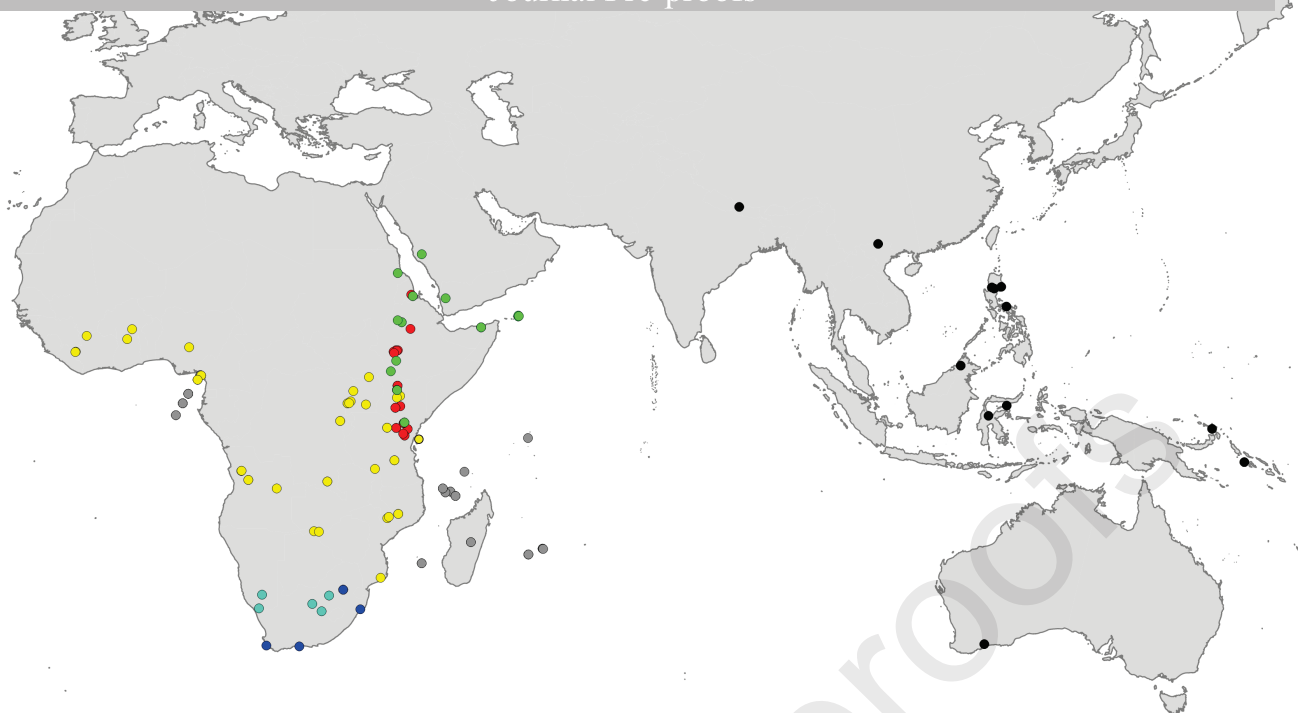
Table 3. Species delimitation of Afrotropical mainland and island birds based on bGMYC (thresholds 0.1-0.9) and GMYC (single- and multi-models), including extra-Afrotropical taxa (included within the phylogeny) for comparative purposes. Grey boxes for extra-Afrotropical taxa correspond to the number of described species (van Balen 2019), while grey boxes for the Afrotropical taxa (mainland and island) represent the preferred thresholds (see Appendix A for discussion).

Threshold or model	bGMYC									GMYC	
	0.1	0.2	0.3	0.4	0.5	0.6	0.7	0.8	0.9	Single	Multi
Mainland	17	19	20	21	24	24	28	34	42	26	27
Island	16	19	20	21	21	22	22	22	22	20	22
Extra-Afrotropical	10	10	10	10	10	10	10	10	11	11	10

Figure 1

A

Journal Pre-proofs



B

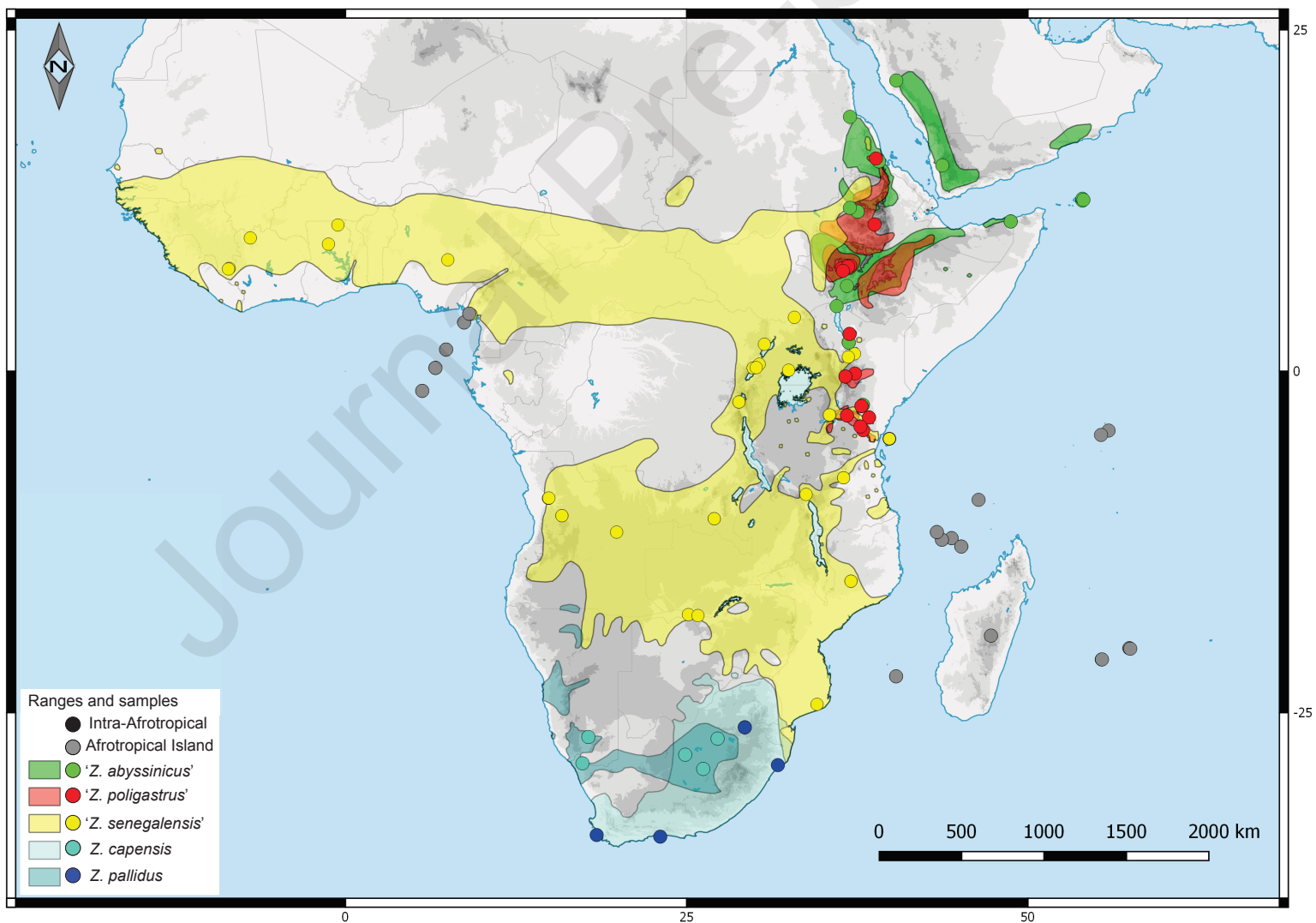


Figure 2

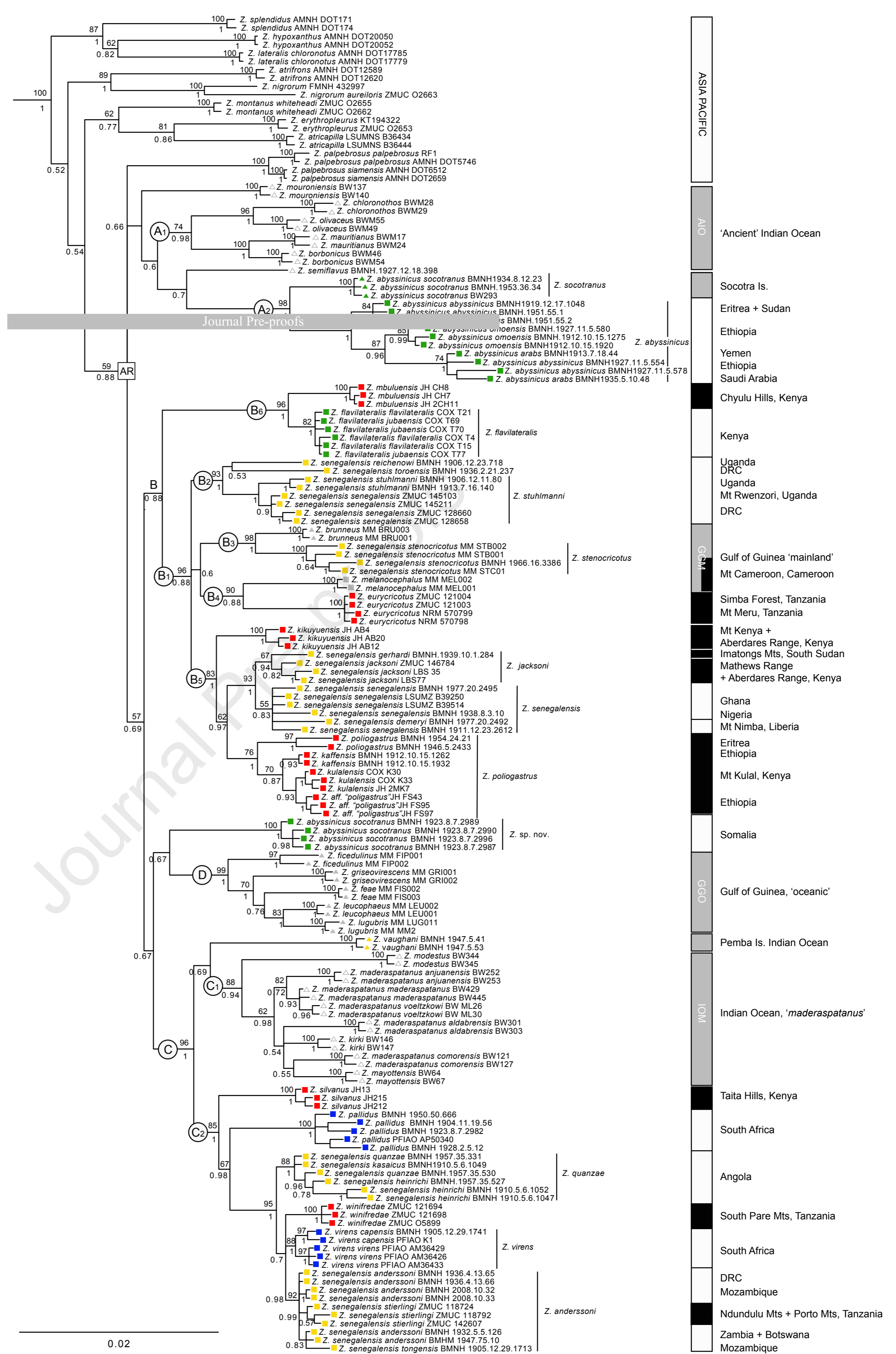
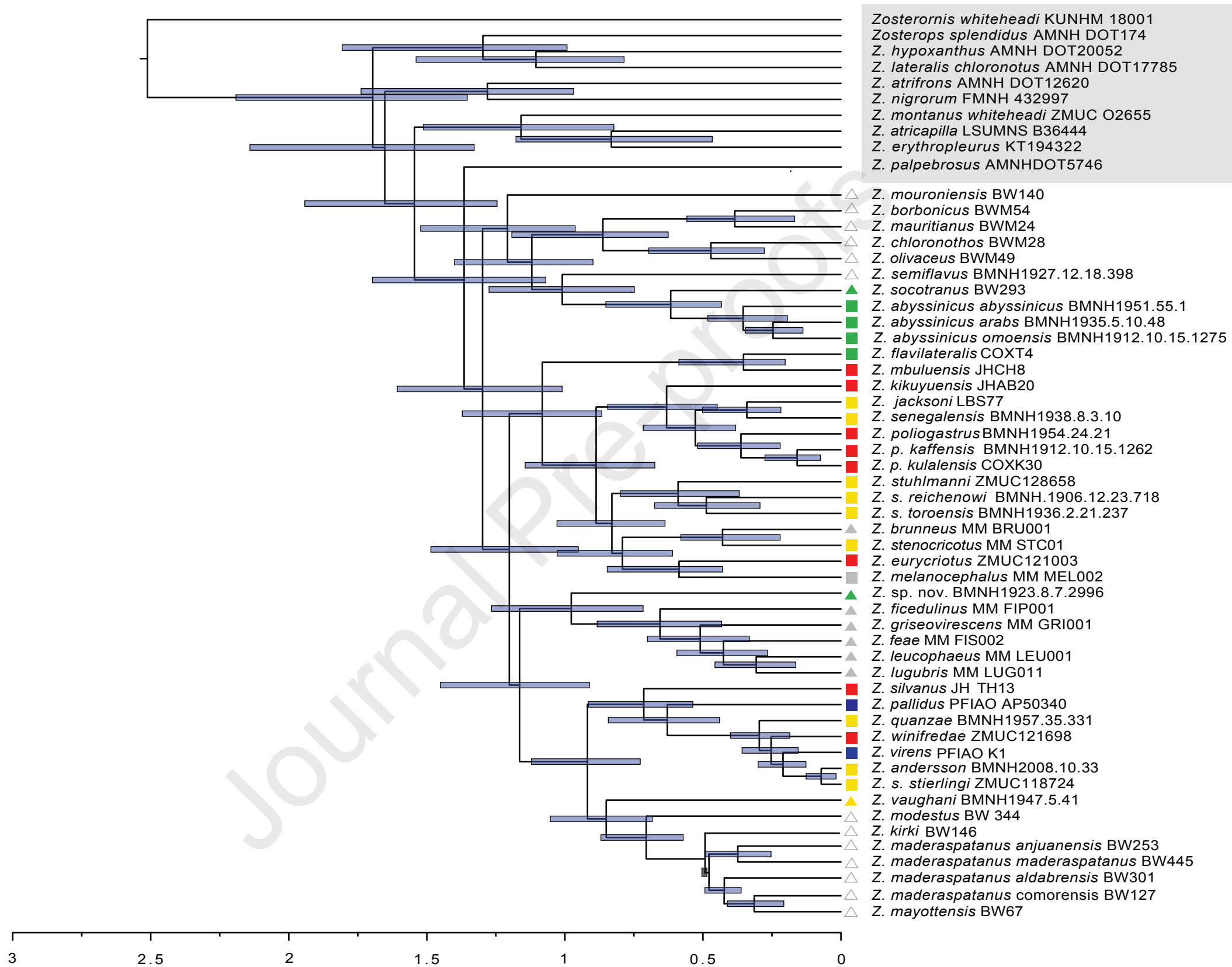


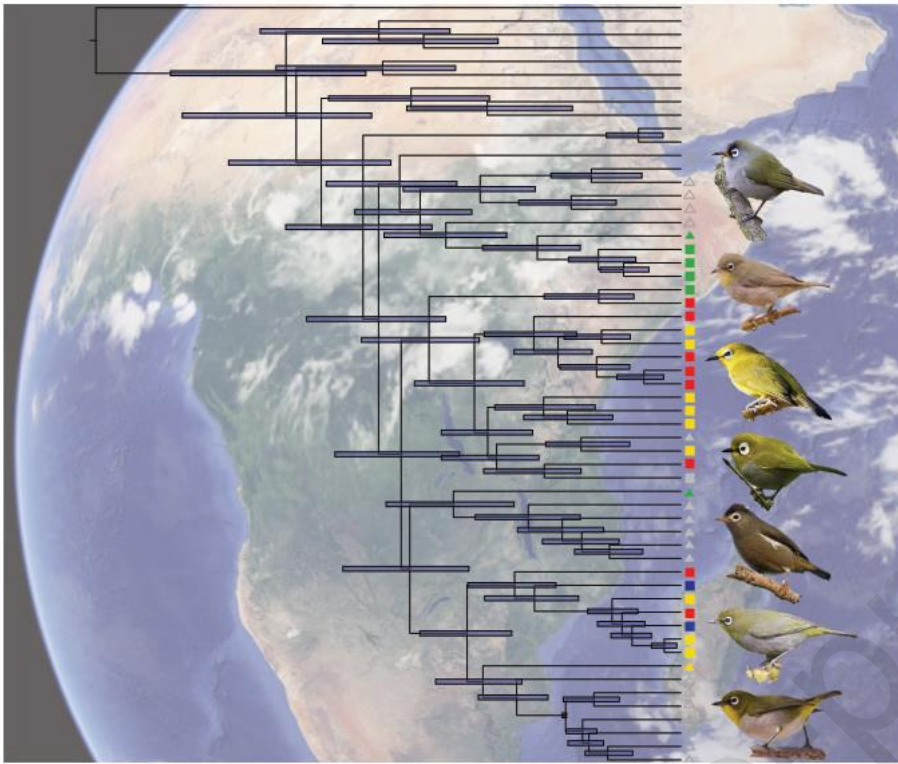
Figure 3



Highlights

- Comprehensive molecular phylogeny of Afrotropical Zosteropidae
- Likely single colonisation of the Afrotropical realm
- Multiple independent colonization of oceanic and ecological islands
- An underestimation of mainland bird diversity
- Proposed revised taxonomy

Journal Pre-proofs



Author statement

Julia Day: Supervision, Conceptualization, Resources, Formal analysis, Writing- Original draft preparation, Visualisation, Data Curation, Project administration. **Frederico Martins:** Investigation, formal analysis, Visualisation. **Siobhan Cox:** Conceptualization, Investigation. **Martin Irestedt:** Investigation, Resources. **Robert P. Prŷs-Jones:** Supervision, Conceptualization, Writing – Review & Editing.

Journal Pre-proofs

Highlights

- Comprehensive molecular phylogeny of Afrotropical Zosteropidae
- Likely single colonisation of the Afrotropical realm
- Multiple independent colonization of oceanic and ecological islands
- An underestimation of mainland bird diversity
- Proposed revised taxonomy

Journal Pre-proofs